Low Intensity Diamond Detector Beam Profiler

Supported by EURISOL – Task 6

M. PÂRLOG

Laboratoire de Physique Corpusculaire de Caen

15.12.2009 – CARAT, GSI

I Introduction:

- *Goal and framework: beam profilers – EURISOL, SPIRAL2, SPARC… & focal plane of the associated spectrometers*

II The synthetic diamond: (properties, fabrication, principle of detection)

- *Single-crystal and polycrystalline sensors*
- *Response and charge collection = f(material quality & thickness, ion Z&E, U)*

III Non-segmented detectors:

- *Construction at LPC and test at GSI (classical electronics) and GANIL (sampling)*
- *Stability of the signal in time; pulse shape analysis (PSA)*

IV Double-sided multi-strip detectors:

- *construction at LPC and tests at GANIL (PSA); analysis in progress*

V Conclusions and prospective

I. Requirements for a (radioactive) beam profiler working below 10^6 pps:

- The **beam profile** (X,Y) - **resolution of 1mm** over an **active area of up to 50x50mm^2**.
- The device should operate at **beam intensities as low as ~1 pps and up to ~10^6pps**.
- The detector should exhibit **a fast rise time** for timing applications (TOF ~0,5 ns) as well as **a short response time** to enable operation at ~10^6 pps.
- The detector should have **a large dynamic range** – both very light and very heavy ions with energies ranging from **a few to ~250 MeV/nucleon** should be detectable.
- The detectors should be **robust and radiation hard** so as to reduce to a minimum their replacement or removal for repair.
- Provide for an **accurate and precise measurement** of the intensity.
- For safety reasons the detectors must have **a good vacuum integrity**.
- **Insensitive to the decay of the radioactive ions** (ie., e-,e+,g , etc).
- From a practical point of view (eg, use by operators during beam tuning) the detectors should be **as simple and straightforward** to operate as possible.

A promising alternative: the large area synthetic polycrystalline diamond (chemical vapour deposition – CVD), have properties matching very closely those needed to fulfil the above requirements

R&D EURISOL Task 6 in LPC and SPARC Task 4.1 at FAIR to determine:

a) the suitability of CVD diamond to detecting heavy ions;
b) The feasibility and testing (by pulse shape analysis) of prototype double-sided strip detectors capable of providing event-by-event position measurement and timing PSA

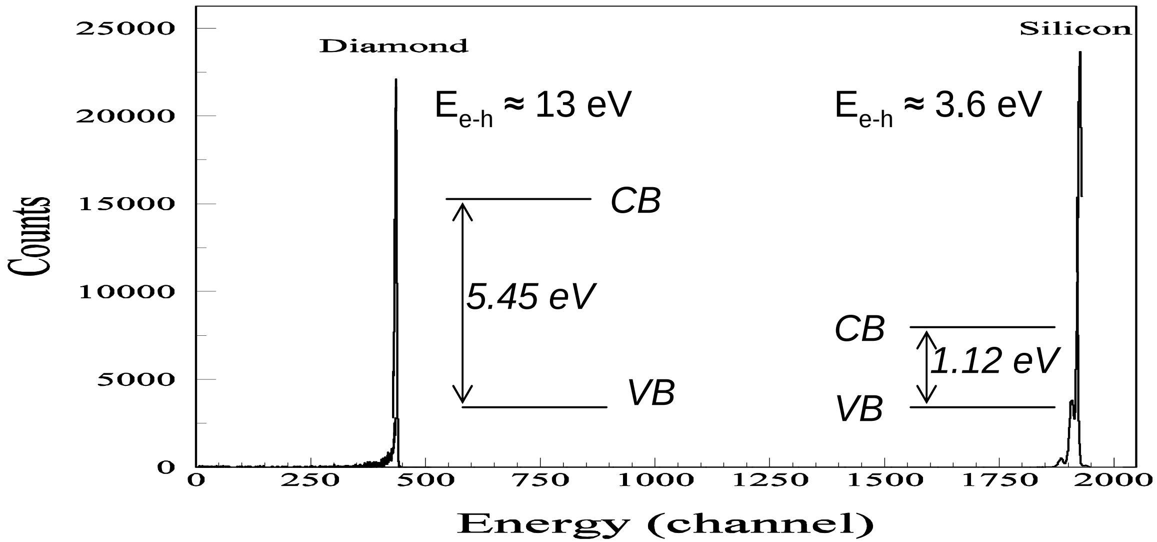

II The CVD diamond detectors may behave in very different ways:

***Single-crystal* diamond** *detector (CEA Saclay) of 20 µm thickness, adaped to the range. (courtesy of J.-L. Lecouey –LPC)*

The signal is 4 lower (left peak) than in a Si detector (right)

^{241}Am: α of 5.5MeV

Range ~15 µm

E.-K. Souw, R.J. Meilunas / Nucl. Instr. and Meth. in Phys. Res. A 400 (1997) 69–86 73

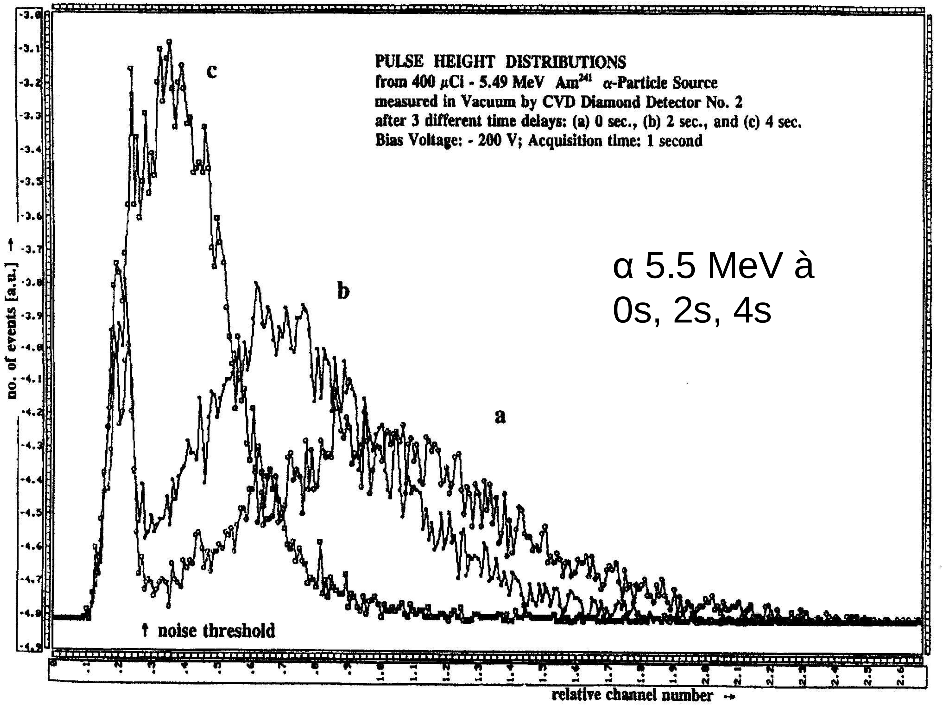

Fig. 3. Pulse height distributions. From 400 µCi–5.49 MeV Am^{241} α-particle source measured in vacuum by CVD diamond detector No. 2 after 3 different time delays: (a) 0 s (b) 2 s and (c) 4 s Bias voltage: −200 V; acquisition time: 1 s. Note, vertical scale is not the same for every PHDs, but individually adjusted to allow a better estimate of PHD peak positions.

***Polycrystalline-crystal* diamond drawback:**

the bulk polarization

Solutions:

- Previous radiation;
- Subbandgap light;
- Electronic procedure;
- Thermic procedure

- Good material!!!
the salutary solution

III Not-segmented detectors: pollycristalline diamond

Cleaning: eau régale + ultra-sounds

($1/5\ H_2O + 3/5\ HCl + 1/5\ HNO_3$)

Electrodes: Au (ageing) or Al;

if not: CrAu, TiAu,)

Contacts: bonding

(Al wire – soldering T + ultra-sounds)

Voltage: ± 1V/ µ or higher

Irradiation: growth face or nucleation face – to be compared

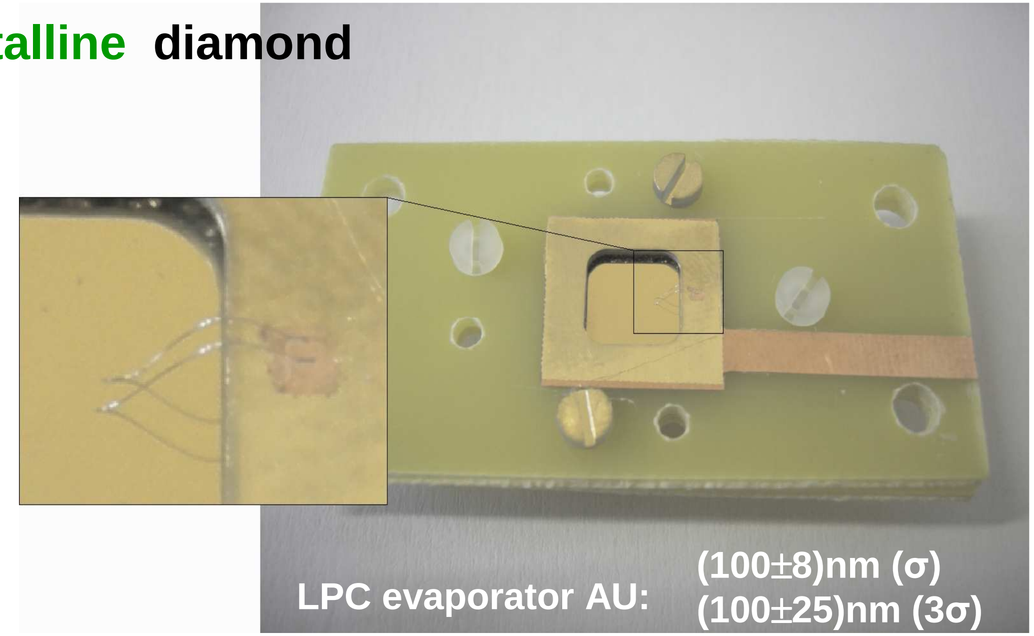

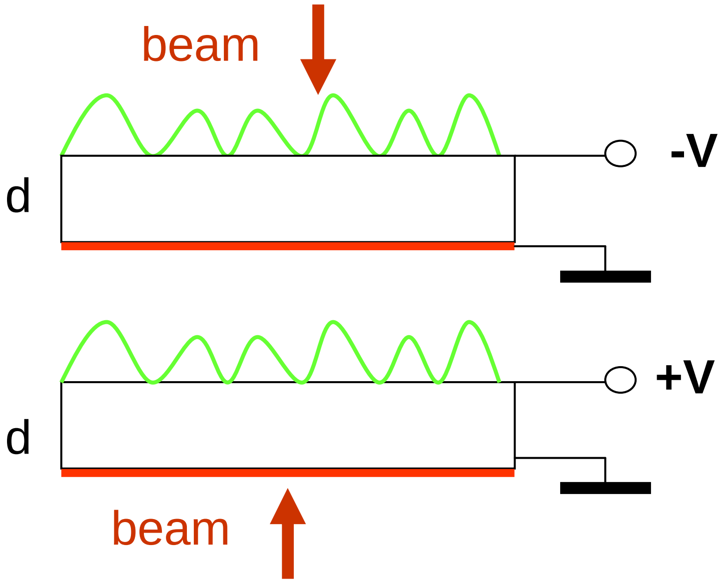

Range<<d: transit electrons

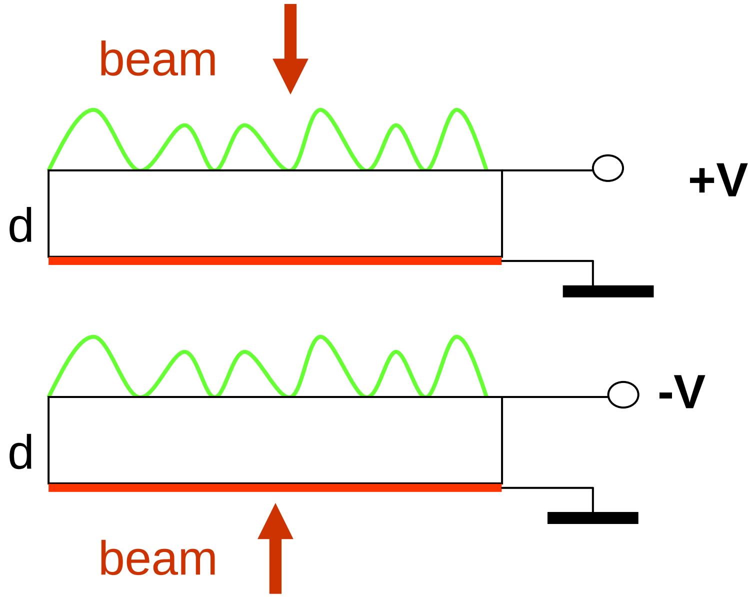

Range<<d: transit holes

Tests of not-segmented detectors in HI beams

Electronics & Acquisition:

GSI:

- classical

GANIL:

- MATACQ – VME (400 MHz BW -> 0,9ns; 2GHz sampling)

- oscillo LeCroy 64Xi (600 MHz BW -> 0,6ns; 10Gs/s)

det1 **Comp1 P1N ELA** 300 µm

det2 **Comp1 P2 ELP** 500 µm

det3 **Company 2** 630 µm

det4 **Company 2** 200 µm

Company 3

det5 165 µm

det6 100 µm

det7 70 µm

Alumine

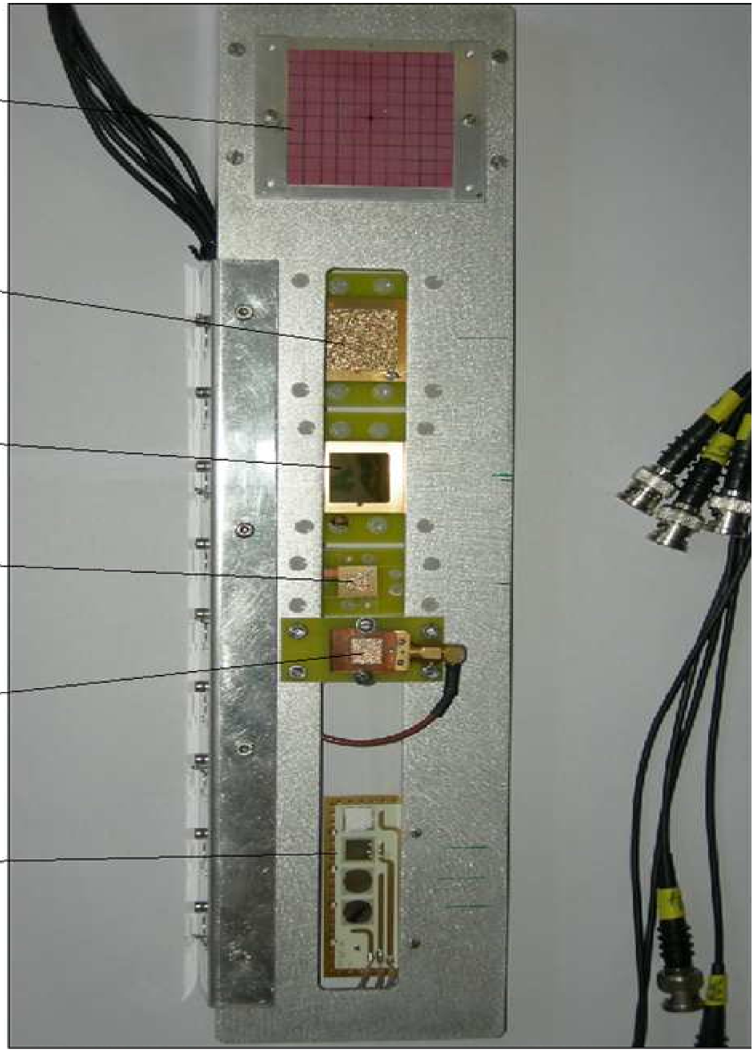

& a 500µ sc tested in 6AMeV 238U beam

Table 1. Energy per nucleon and range of the ions which have served to test the uni-strip diamond detectors.

~50 m	GSI ^{124}Xe	GANIL ^{58}Ni	GANIL ^{13}C	GANIL ^{13}C	LPC α
E/A (MeV)	50	10.9	11.1	7.3	1.2
Range (µ)	440	63	196	98	15

A. Bräuning Demian arguments ε=100%

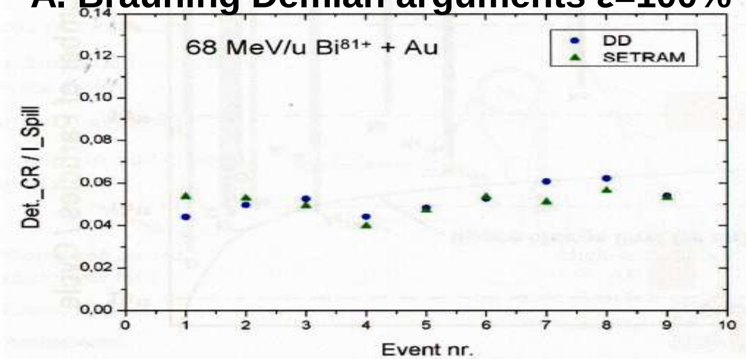

6.2 GeV ^{124}Xe (3.4 GeV in 300 μ)

GSI: ~3*10^7p/spill; runs of a few min, for hours

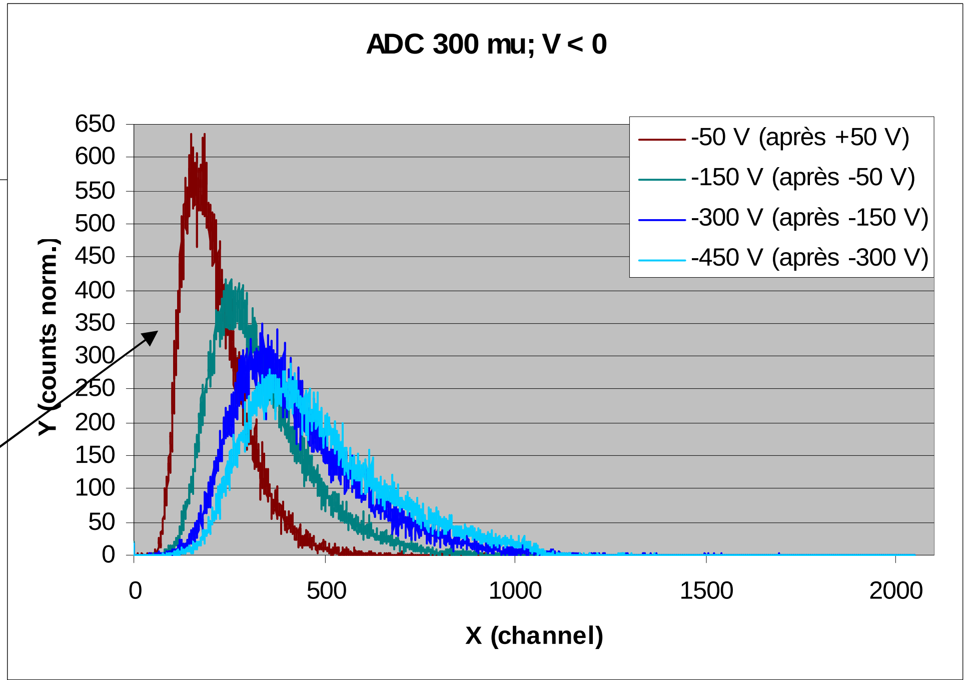

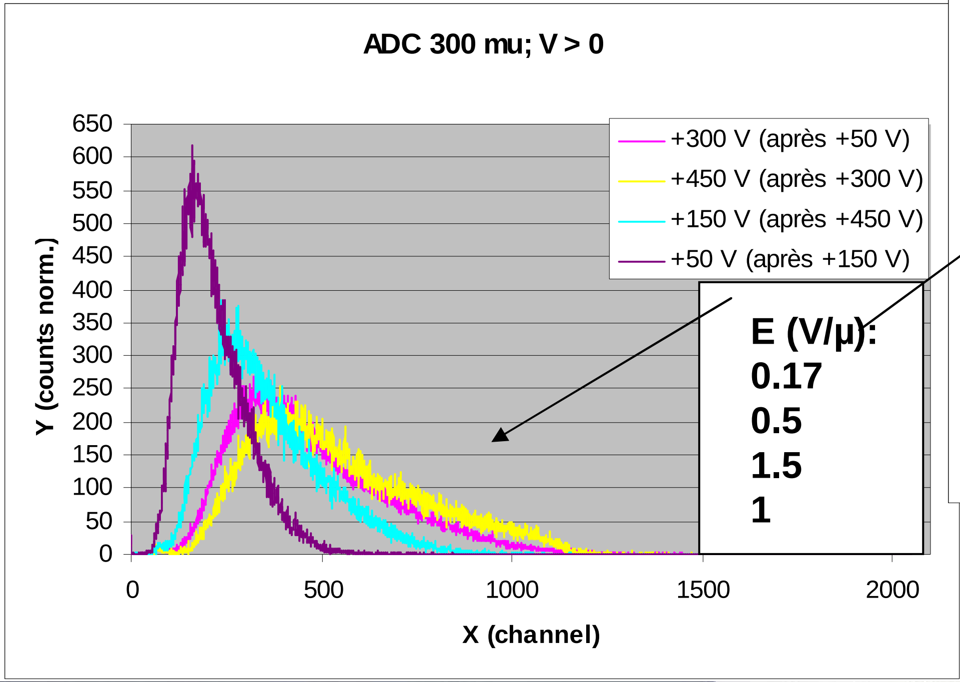

Amplitude spectra: the distribution becomes narrower when the electric field diminishes.

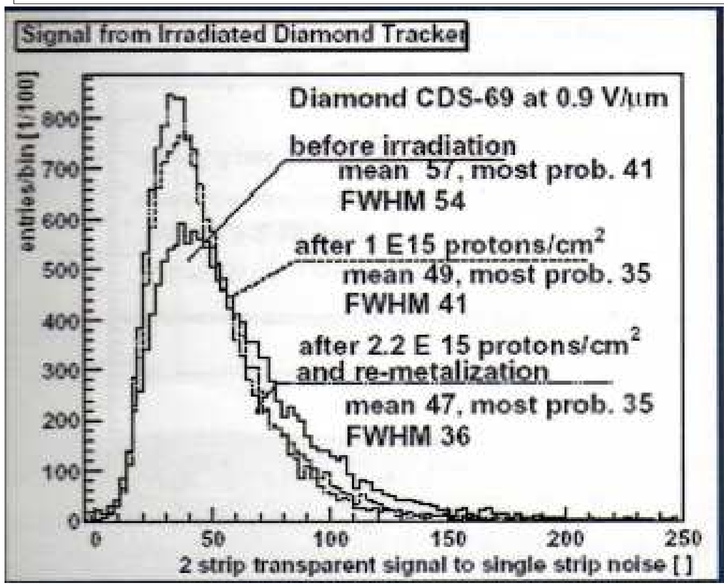

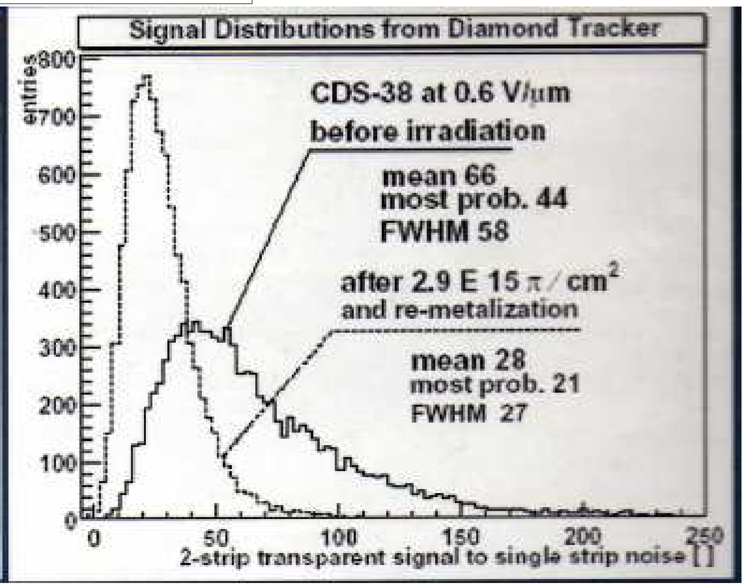

P. Delpierre, RD 42
Journées de prospective du CPPM, 2006

Conjecture: during the irradiation, the electric field may diminish due to the progressive bulk polarization.

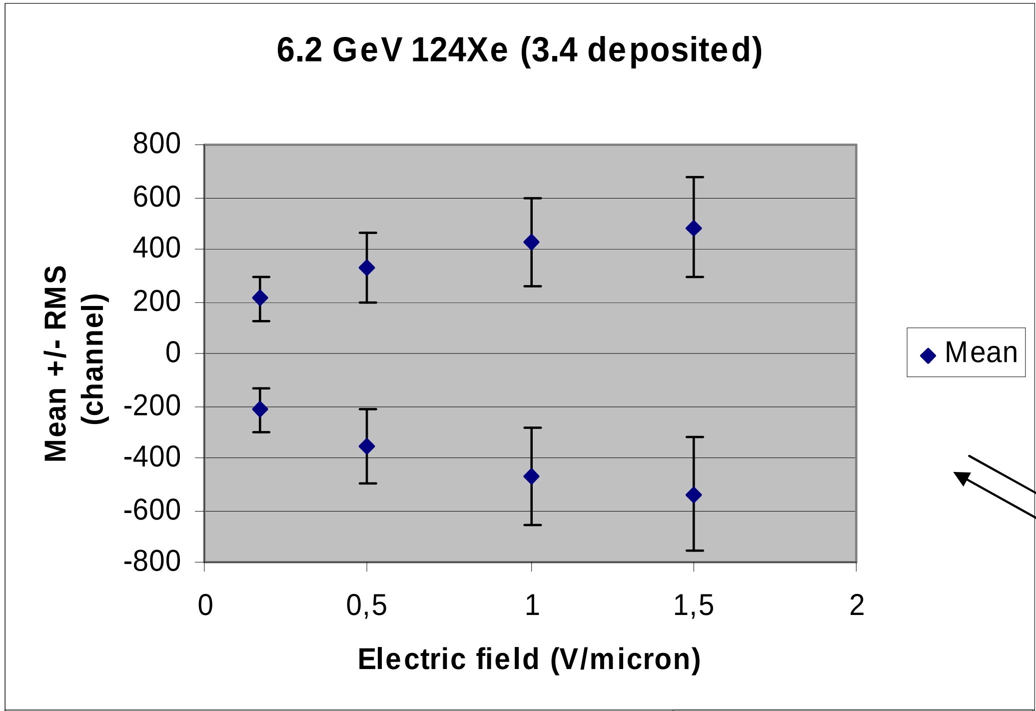

Slightly better collection (~10%) for U > 0, i.e. when the holes coming from the higher carrier density have a shorter drift road.

The relative RMS (%) remains practically the same

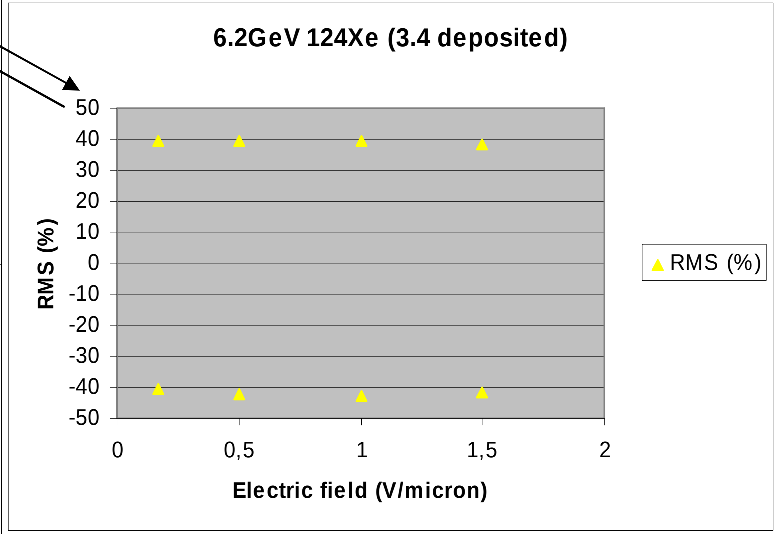

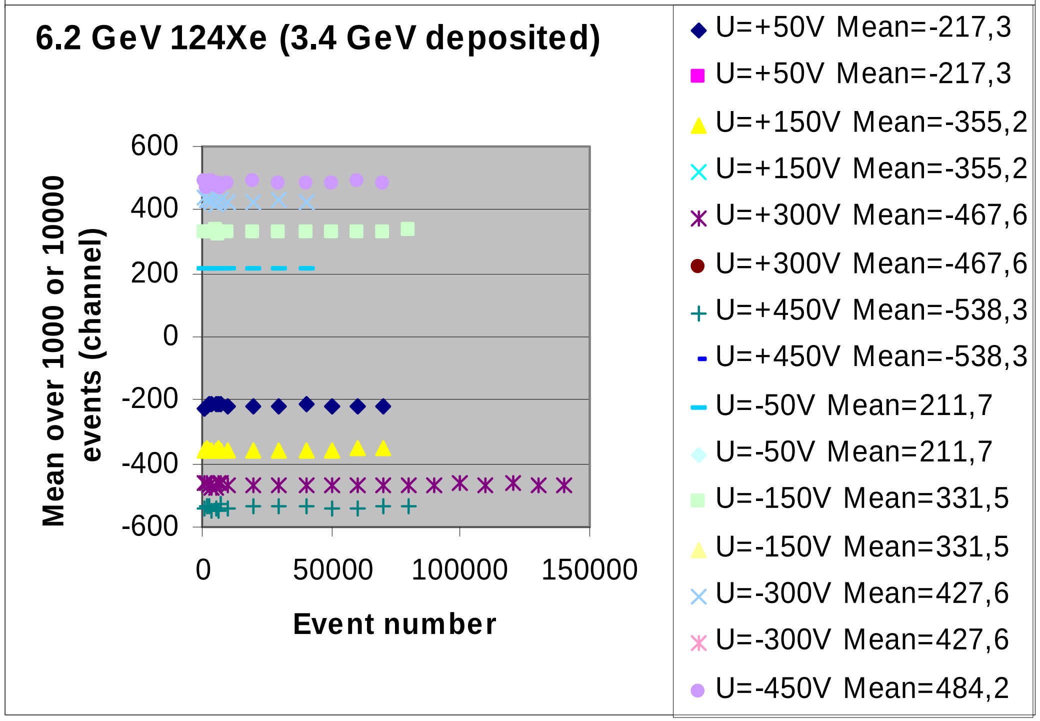

Groups of 1000 or 10000 events, chronologically taped, show the same distribution ==> no signal attenuation observed

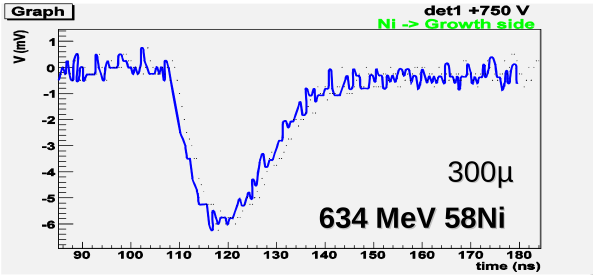

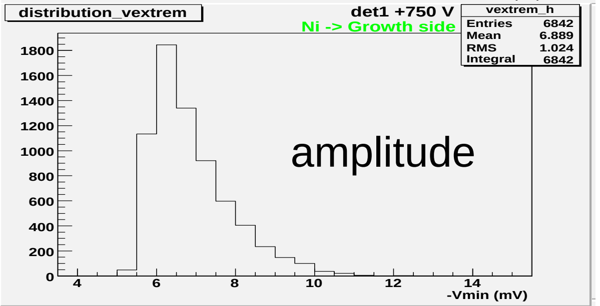

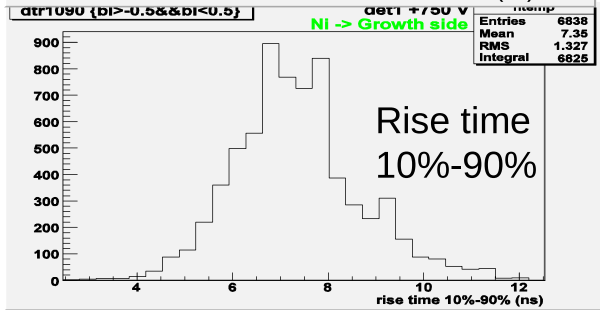

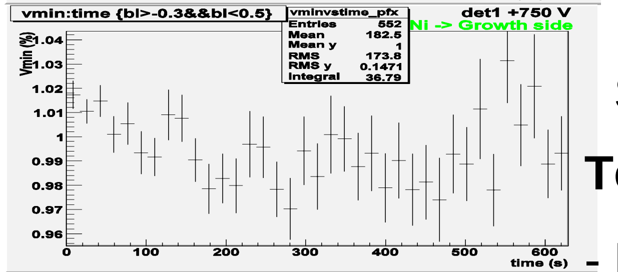

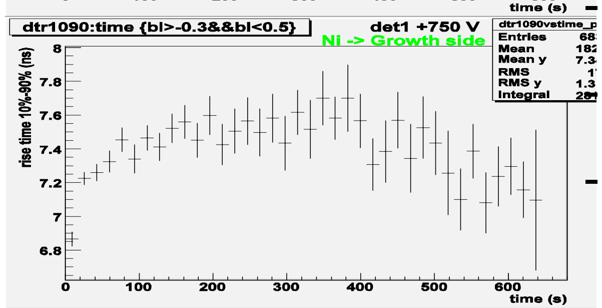

d - thickness; R – range: R<<d

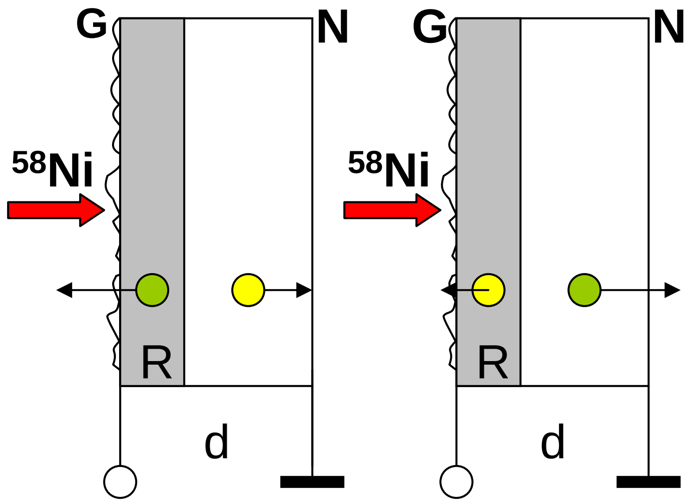

+750V **-750V**

$0 \leq S_e \leq R$

$d\text{-}R \leq S_h \leq d$

$0 \leq S_e \leq R$

$d\text{-}R \leq S_h \leq d$

favorable

S_e – drift **électrons -**

S_h – drift **holes +**

Tests - not-segmented detectors:

- $\text{Proba}_{trapping}$ h > $\text{Proba}_{trapping}$ e

$S_h < S_e$ – favorable

E=2,5V/µ

- d adequate to R

GANIL – SME: ~10^4 pps

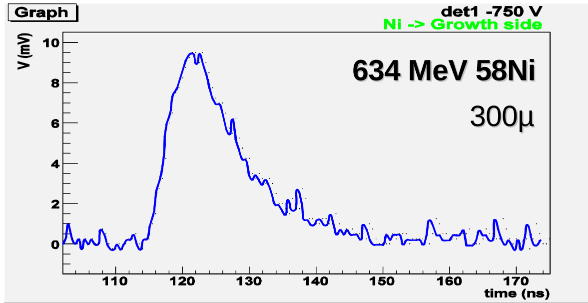

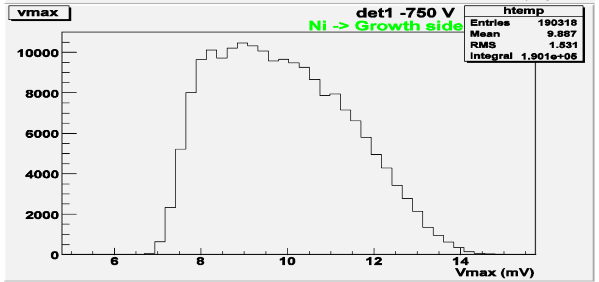

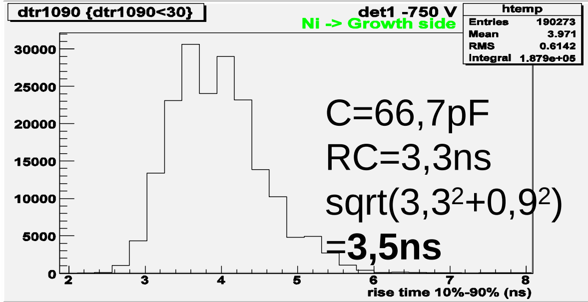

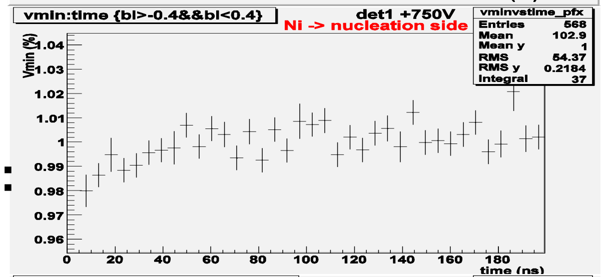

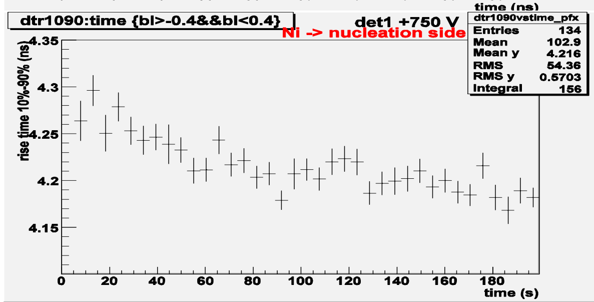

300 μ; E = 2,5 V/μ

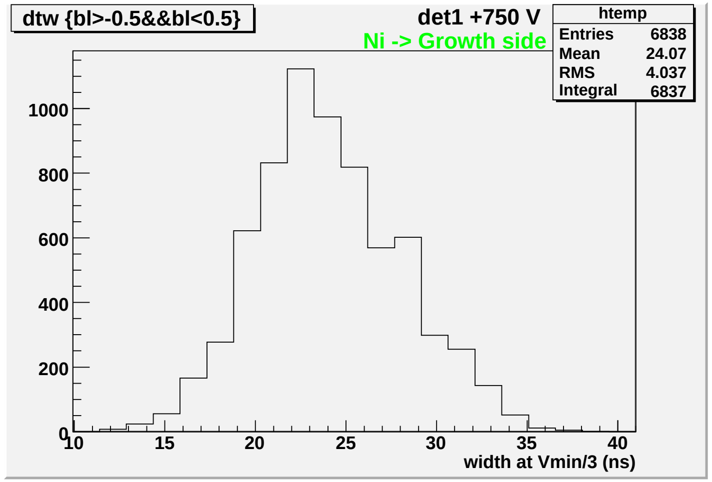

Width at 1/3Vextrem (ns)

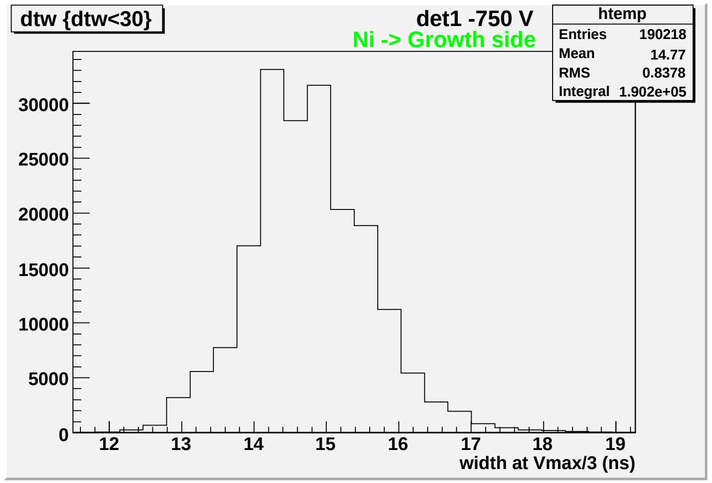

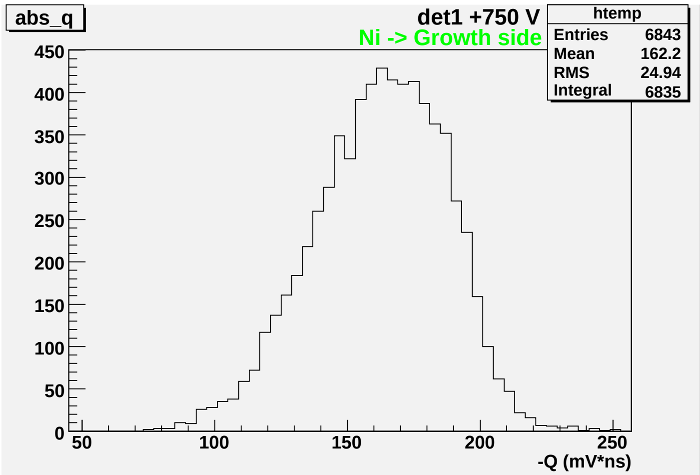

Charge (mV*ns)

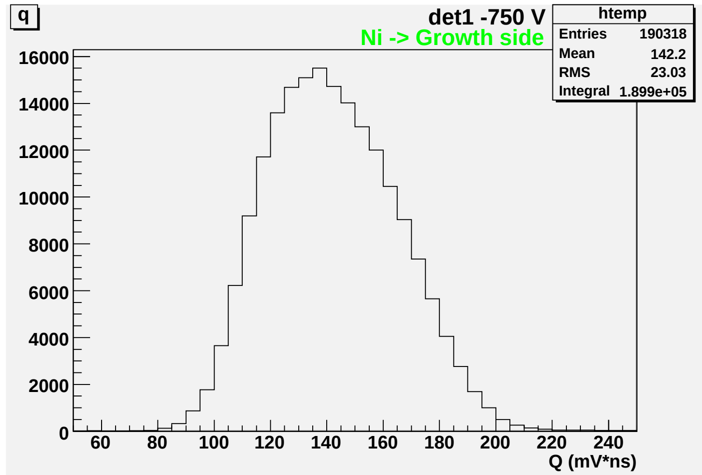

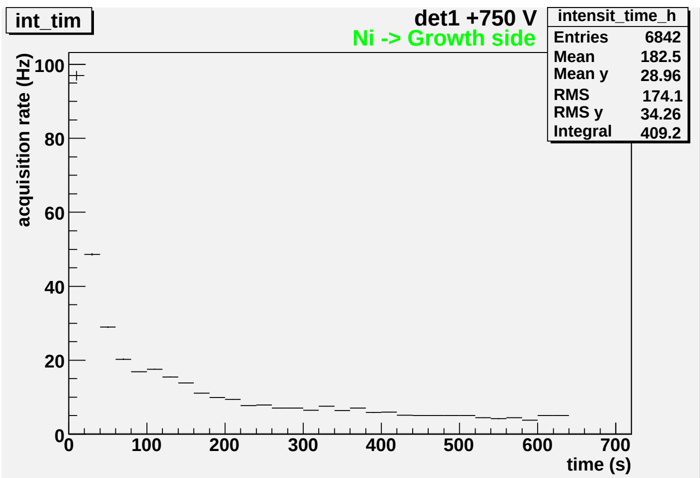

Acquisition rate (Hz)

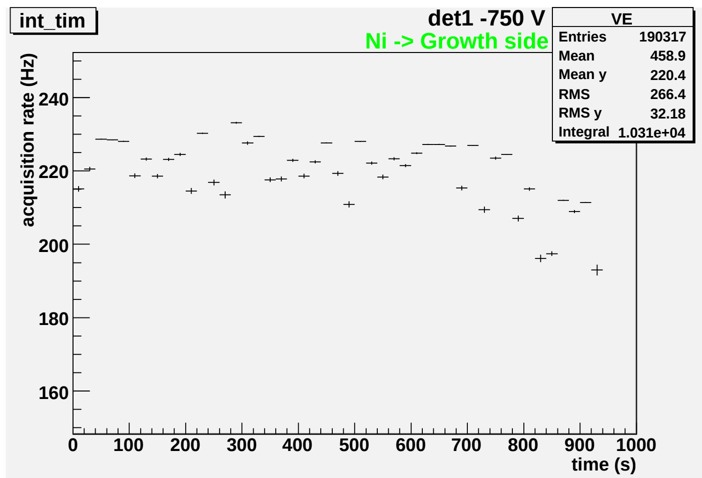

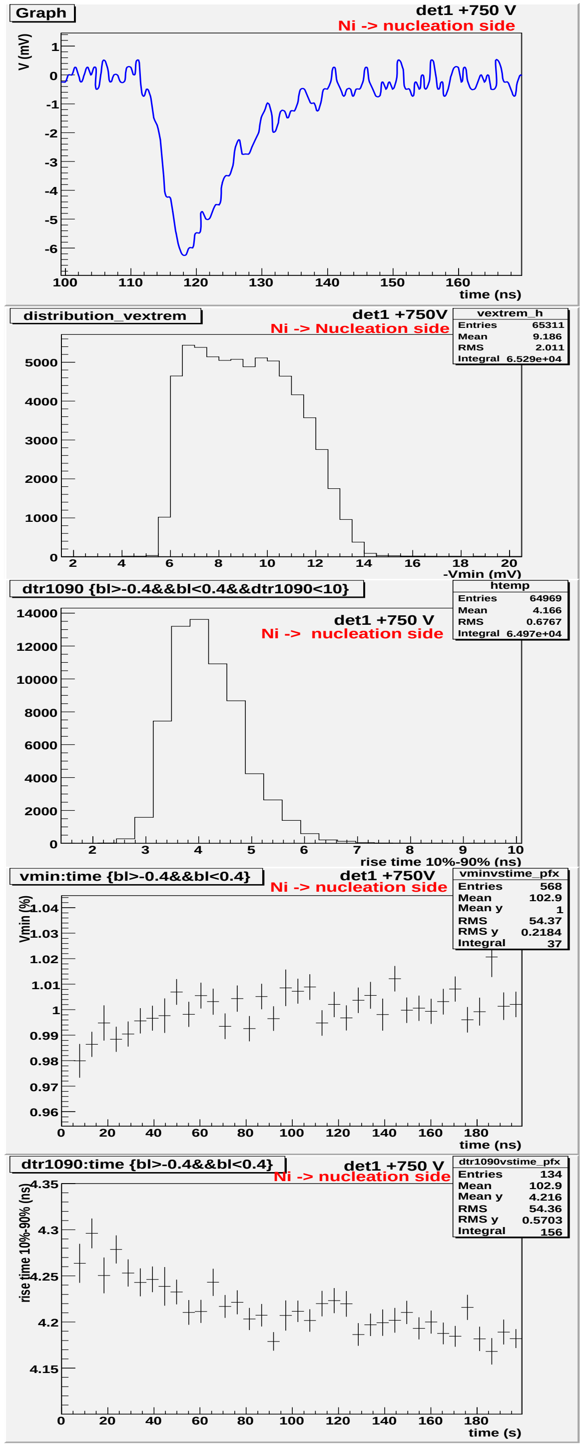

d - thickness; R – range: R<<d

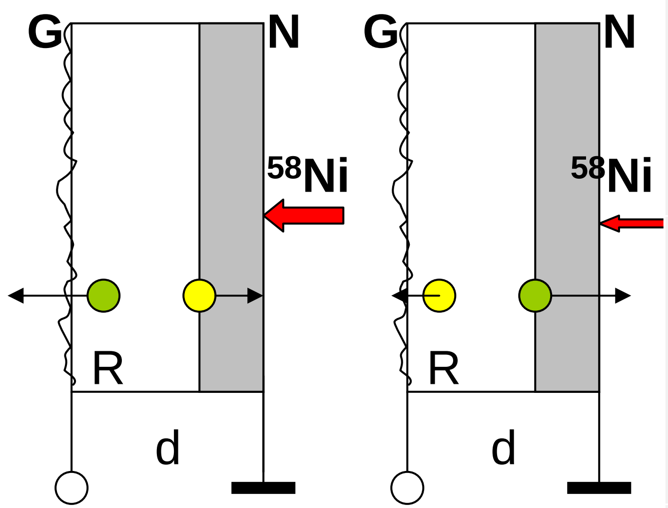

+750V	**-750V**
$0 \leq S_h \leq R$	$0 \leq S_e \leq R$
$d-R \leq S_e \leq d$	$d-R \leq S_h \leq d$
favorable	

S_e – drift **électrons -**

S_h – drift **holes +**

Tests - not-segmented detectors:

- $Proba_{trapping}$ h > $Proba_{trapping}$ e
- $S_h < S_e$ – favorable
- d adequate to R

GANIL – SME: ~10^4 pps

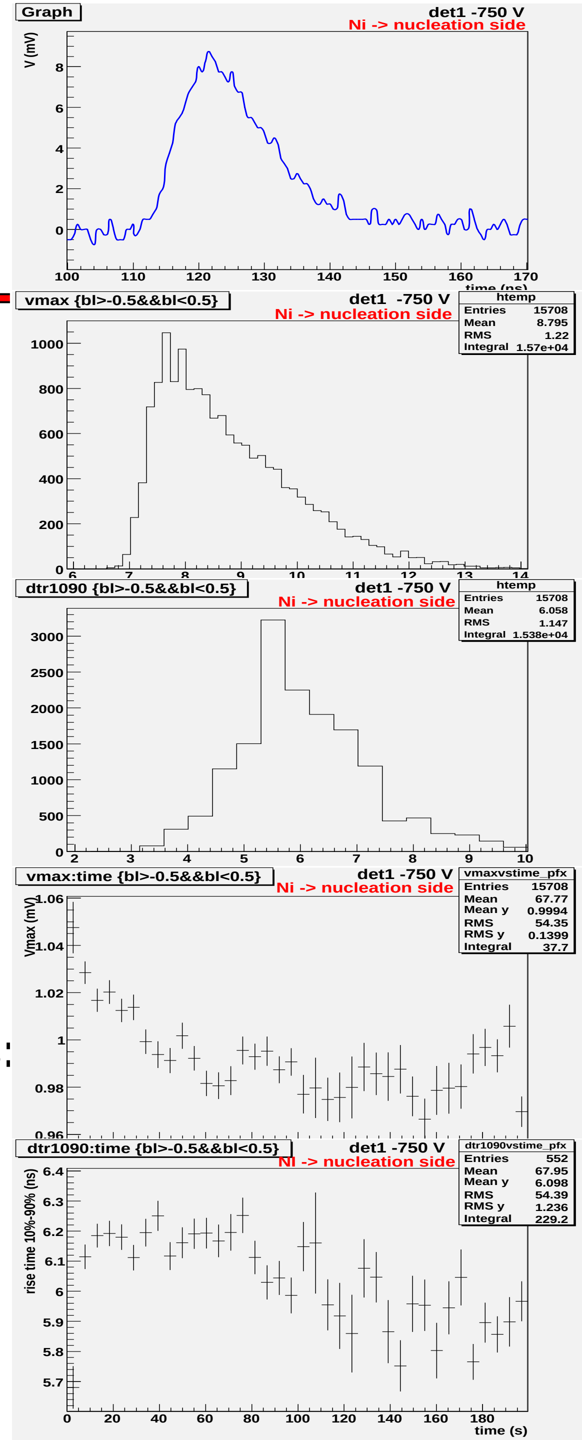

300 μ; E = 2,5 V/μ

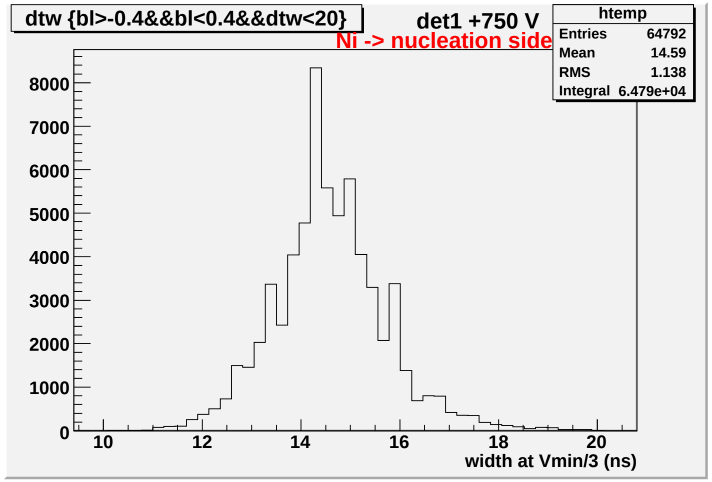

Width at 1/3Vextrem (ns)

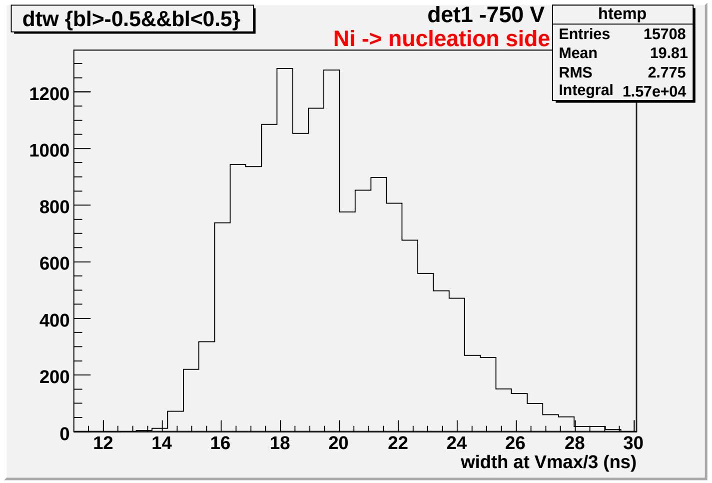

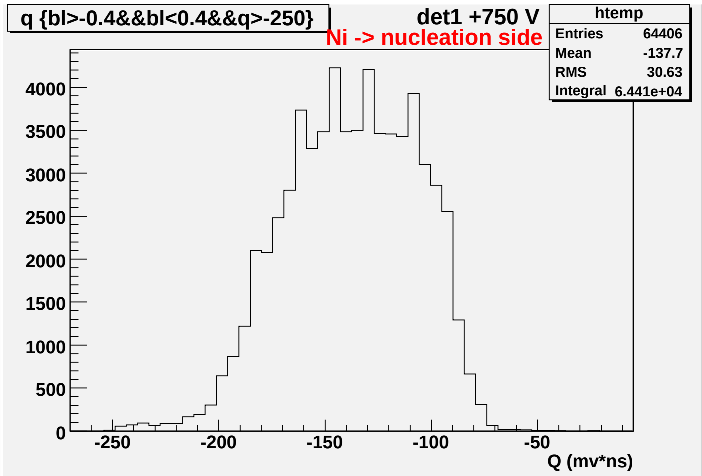

Charge (mV*ns)

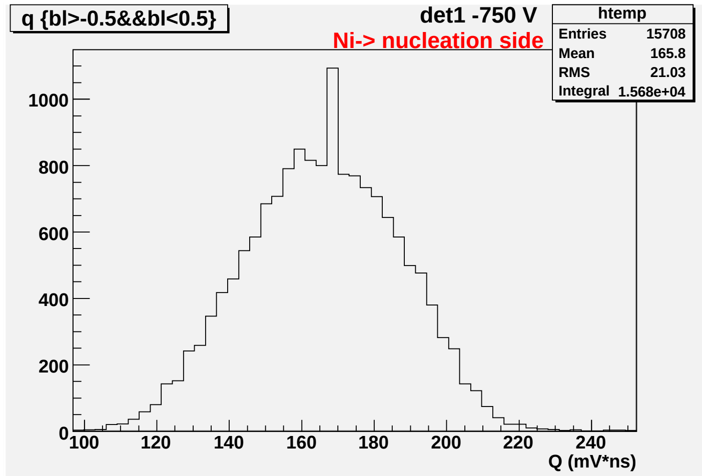

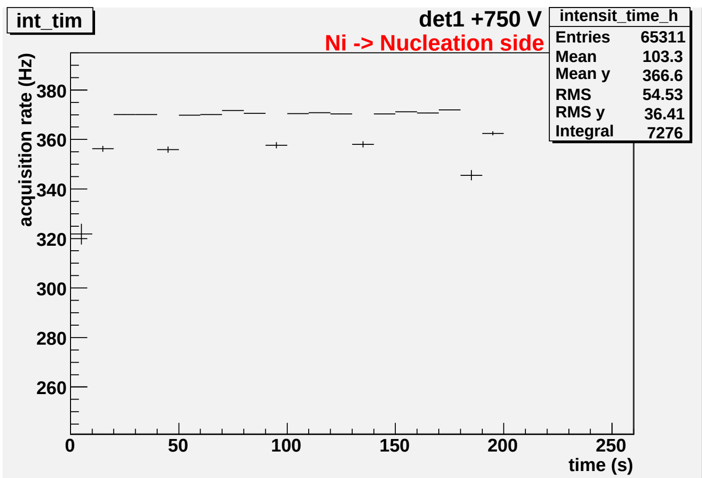

Acquisition rate (Hz)

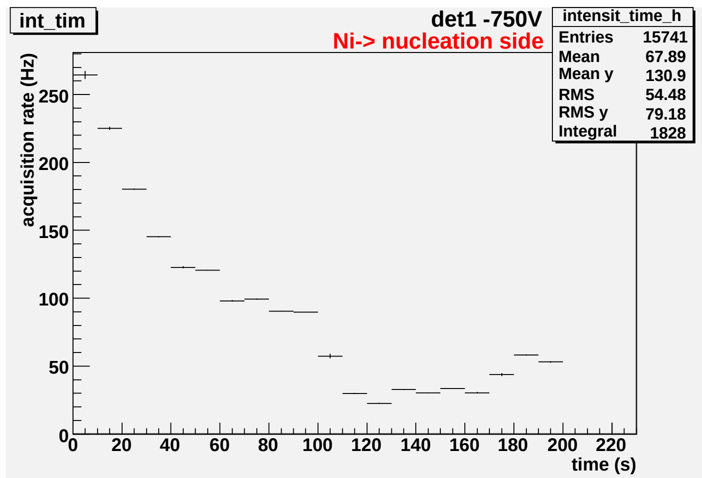

Table 3. Synthetic results concerning the shape of the signal induced by **634 MeV ^{58}Ni** ions, having a **range of ~ 60 µm** in a uni-strip diamond detector **P1N ELA of 300 µm** at **E = 2,5 V/µ** .

irradiated face	**G face U (V) long tranzit**	$\langle V_{extrem} \rangle$ (mV)	Rms V (mV)	$\langle Q \rangle$ (mV*ns)	Rms Q (mV*ns)	tr (ns)	rms tr (ns)	$\langle w_{1/3} \rangle$ (ns)	Rms w (ns)
G	+750 holes	6.9	1.0	162	25	7.4	1.3	24.1	4.0
G	-750 electrons	9.9	1.5	142	23	4.0	0.61	14.8	0.84
N	+750 electrons	9.2	2.0	138	31	4.2	0.68	14.6	1.1
N	-750 holes	8.8	1.2	166	21	6.1	1.1	19.8	2.8

The important conclusion emerging from Table 3 is that, **when the range of the ion is much shorter then the detector thickness**, so that the lengths of the distances of drift of the two types of carriers in their path to the electrode that will collect them are different, **the voltage has to be chosen in such a way that the holes have the shortest drift road,** regardless of the irradiated face. This will have several beneficial effects: the signal amplitude will be greater, because the charge carrier collection will be better, the signals will be shorter, being characterized by a faster rise time and a shorter duration. The quality of the signals, somehow better on the fourth line of the table as compared to that on the first line - both of them concerning the long drift distance for the holes – may show that **the probability of hole catching is a little bit smaller when their road leads to the growth side**, with bigger diamond crystallites and therefore a higher quality (for the fourth line) than when their road leads towards the nucleation side, enclosing more graphite (first line).

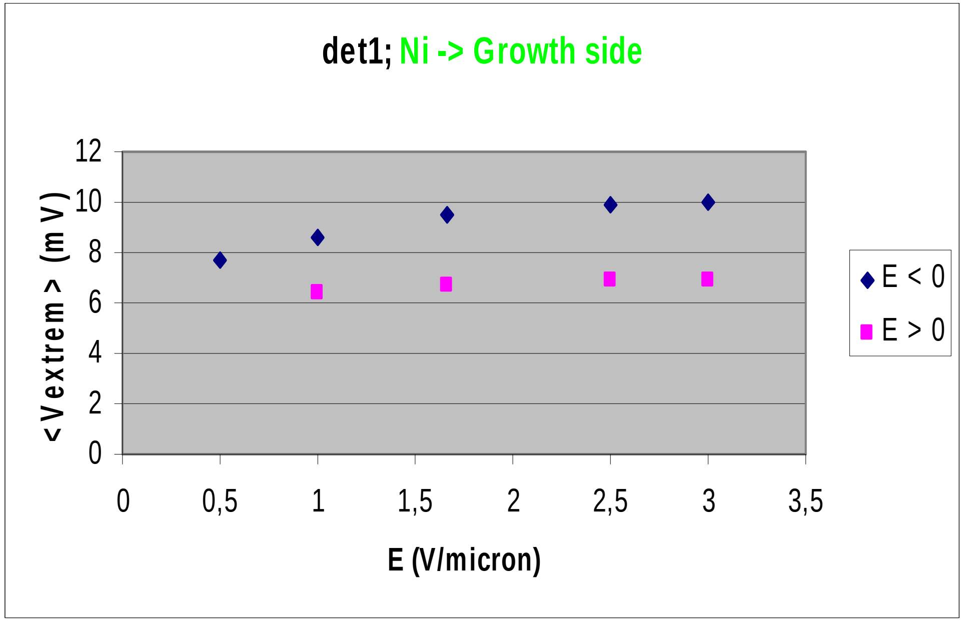

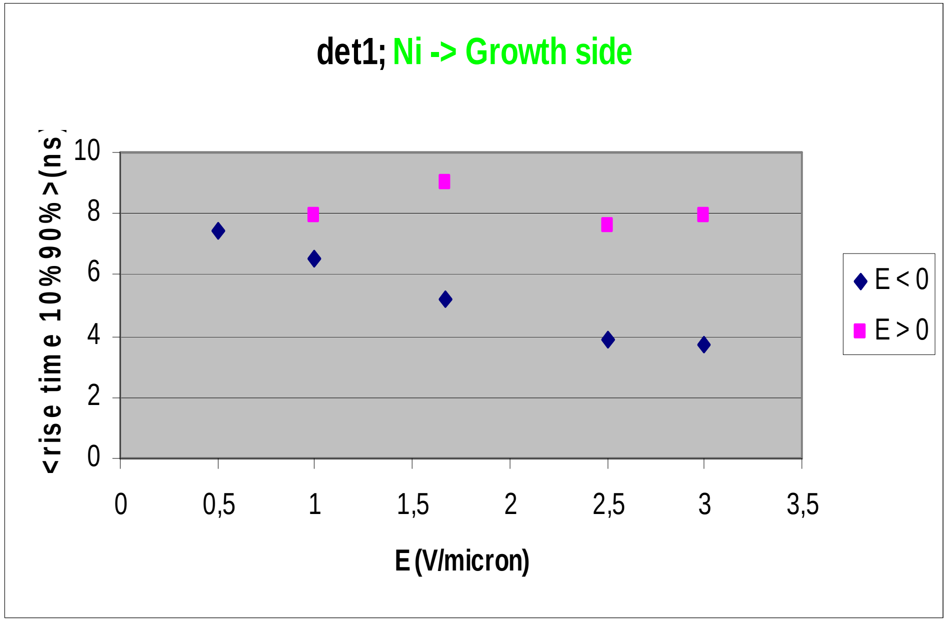

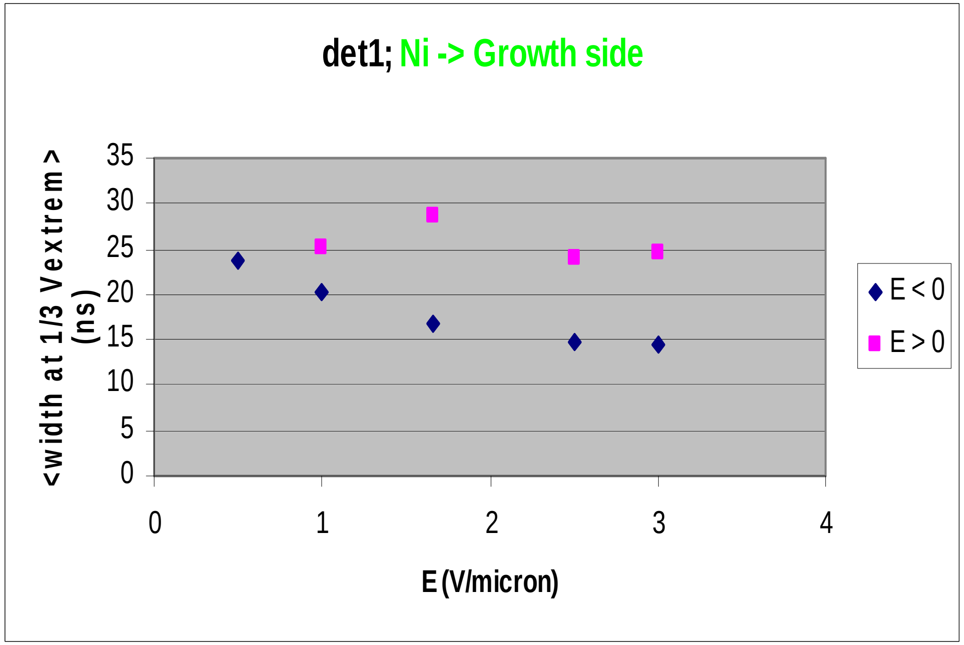

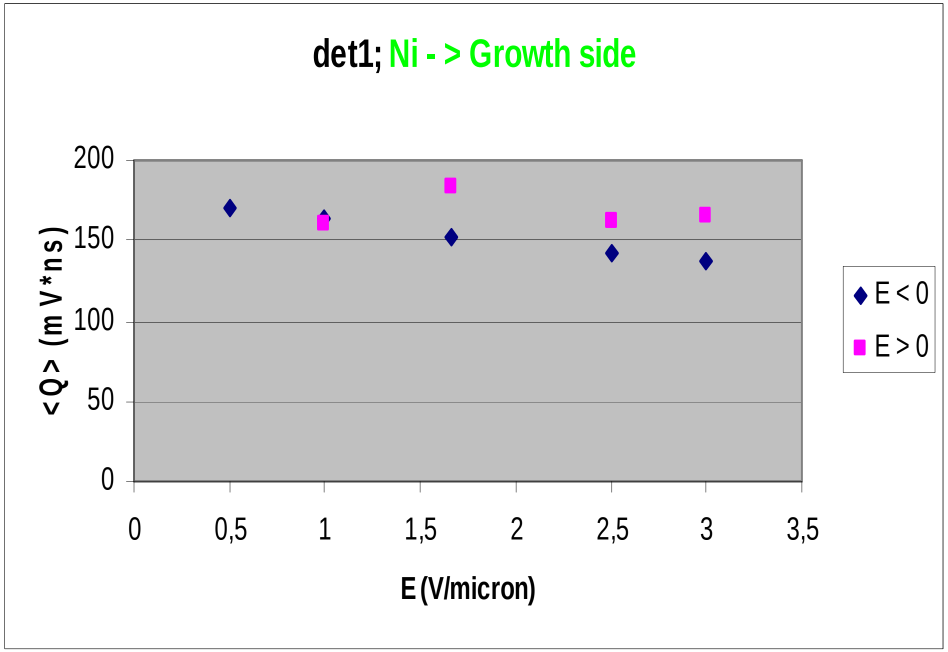

When R<d, the signal is higher and faster when the **electrons** drift on a **longer** way then the **holes**.

Similar results for det2

^{58}Ni: 10.9 AMeV

PSA: Different detectors, different behaviors

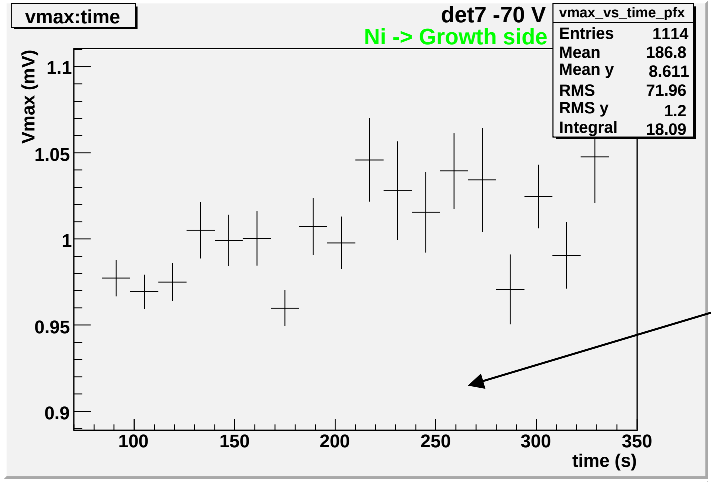

E=1V/μ

70 μ, Company 3

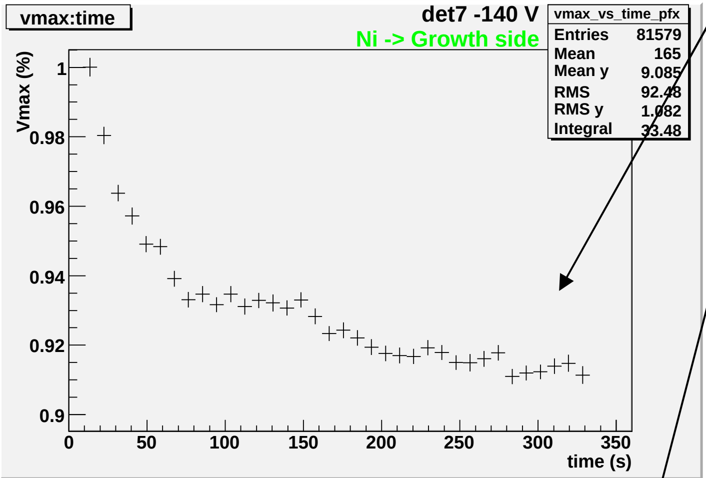

E=2V/μ

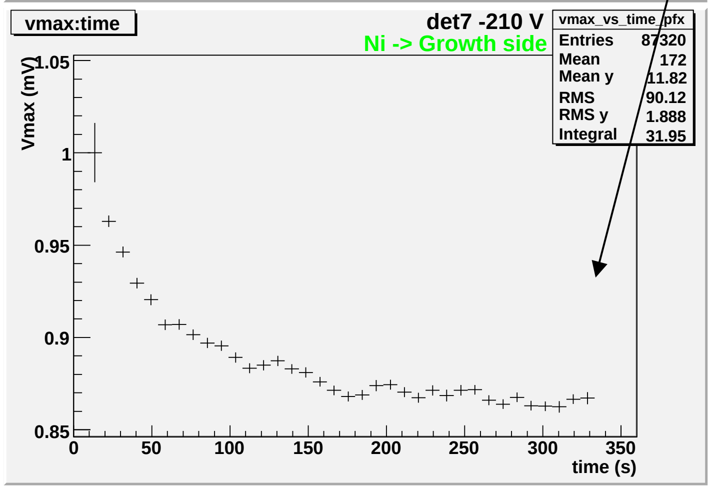

E=3V/μ

200 μ, Company 2

E=2.5V/μ

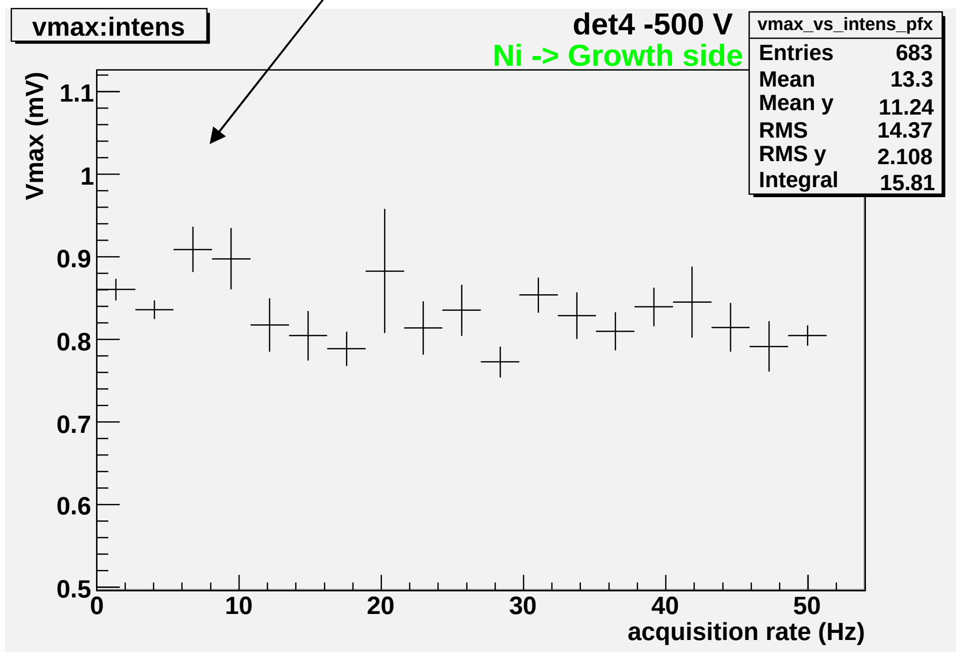

IV Multi-strip detctors: Company 1 - ELP vs ELS

ELP (Electronic Premium Grade) – processed from a polycrystalline wafer with a starting thickness of 1 mm; the final thickness is achieved by removal from the nucleation surface; therefore, thinner the thickness of an ELP plate is, higher its quality; but under 0.2 mm, the risk of breaking in the process of lapping and polishing is much increasing;
ELS (Electronic Standard Grade) – processed from a polycrystalline wafer with a minimum removal of 100 µm. Comparing the two types of material was one of the objectives of our study.

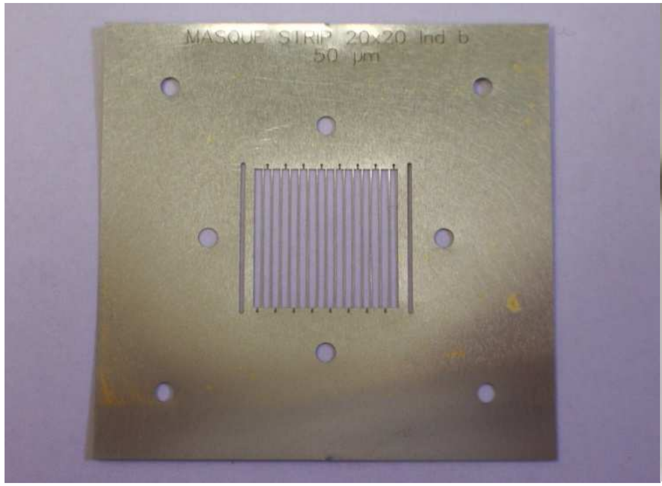

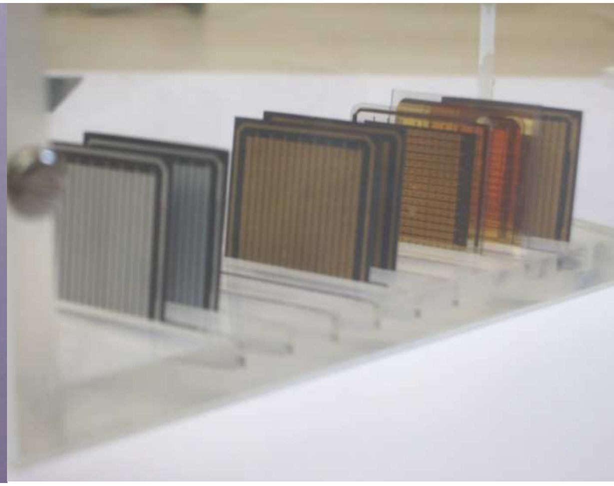

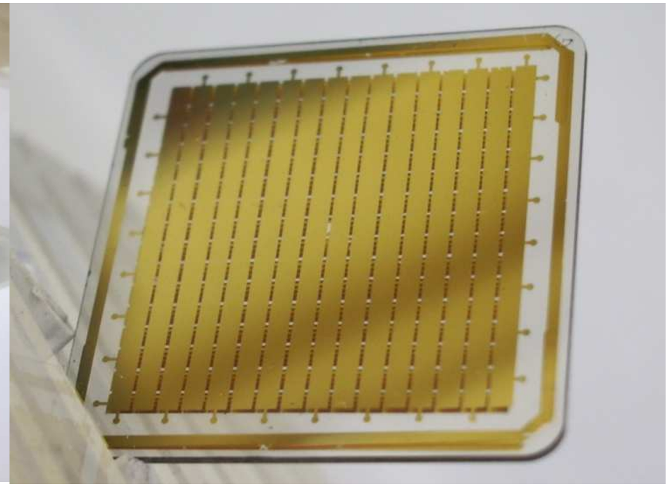

Strip pitch: 0.9mm inter-strip gap: 0.1mm
efficiency: 90%

The BERGER files for the masks & PCBs were done at LPC

Flange and connectors

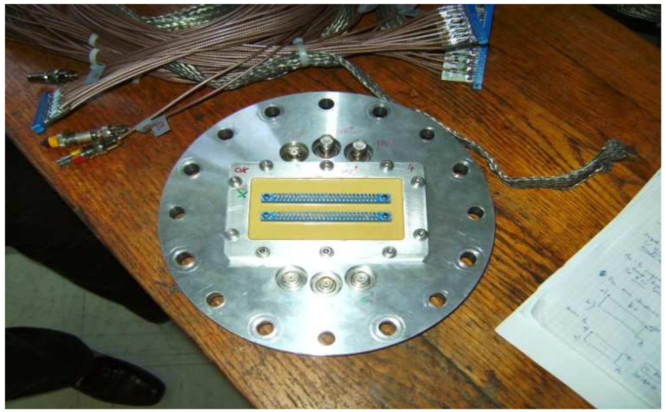

Det III:

5.5 MeV α

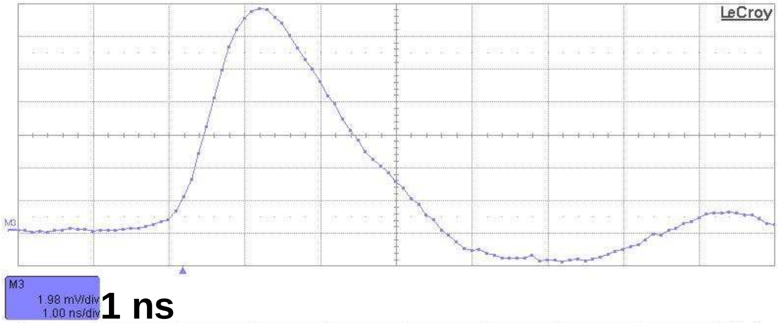

1 ns

PRL: developped at LPC

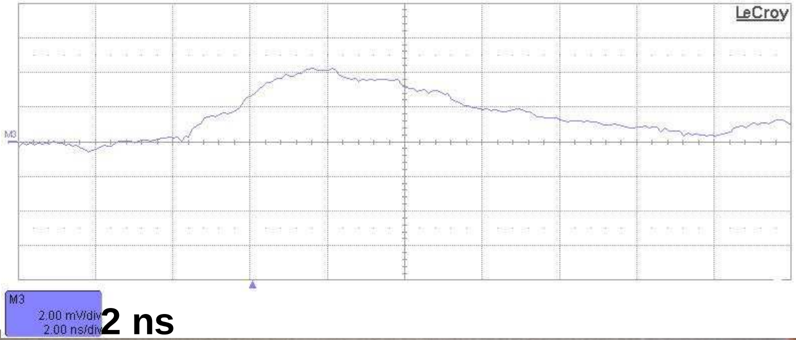

2 ns

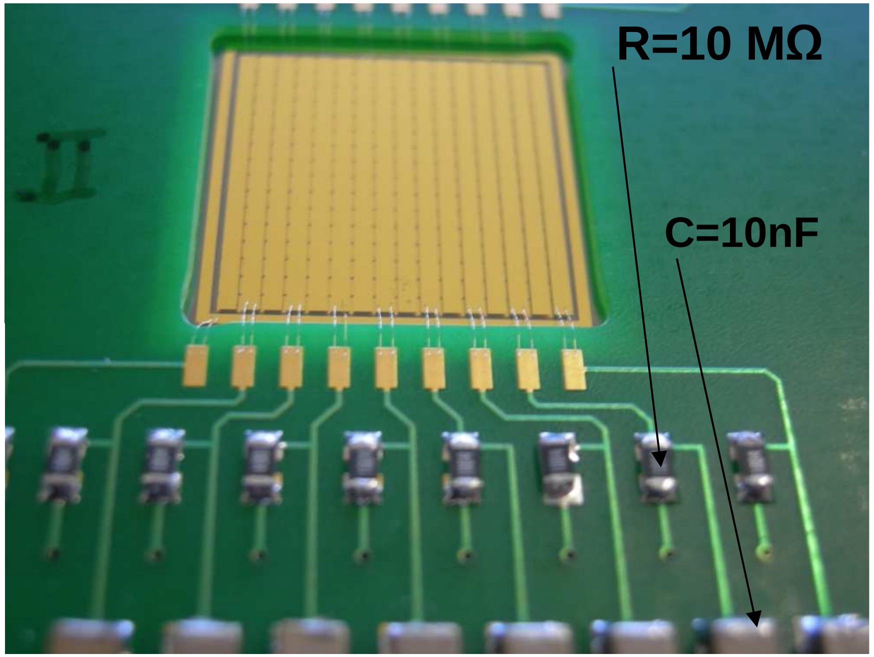

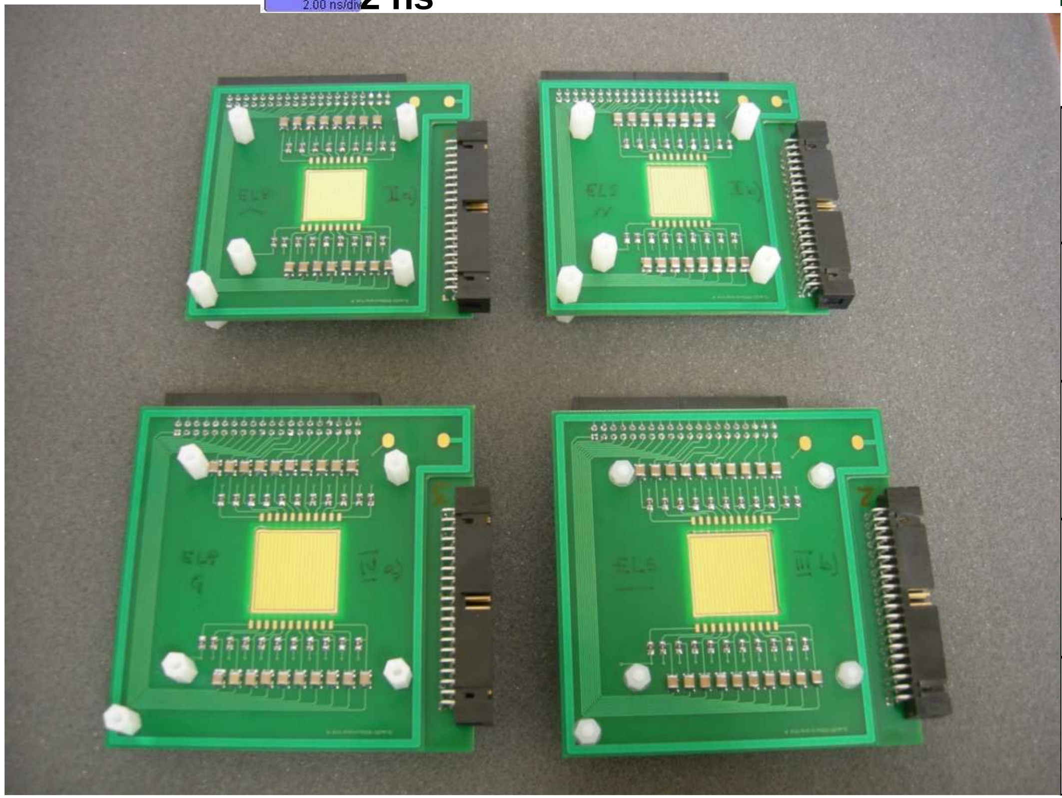

Table 3. the multi-strip detectors built at LCP; a) and b) are the 2 faces

Detec teur	P2 - Type	Densité (g/cm3)	Epaisseur (μm)	Surface active (mm x mm)	Nombre de pistes
I	ELS	2.9	565	16 x 16	a) 16 b) 16
II	ELP	3.4	575	16 x 16	a) 16 b) 16
III	ELS	2.9	240	20 x 20	a) 1 b) 20
IV	ELP	3.4	350	20 x 20	a) 20 b) 20

Les tests au GANIL: sur la ligne SME (sortie moyenne énergie)

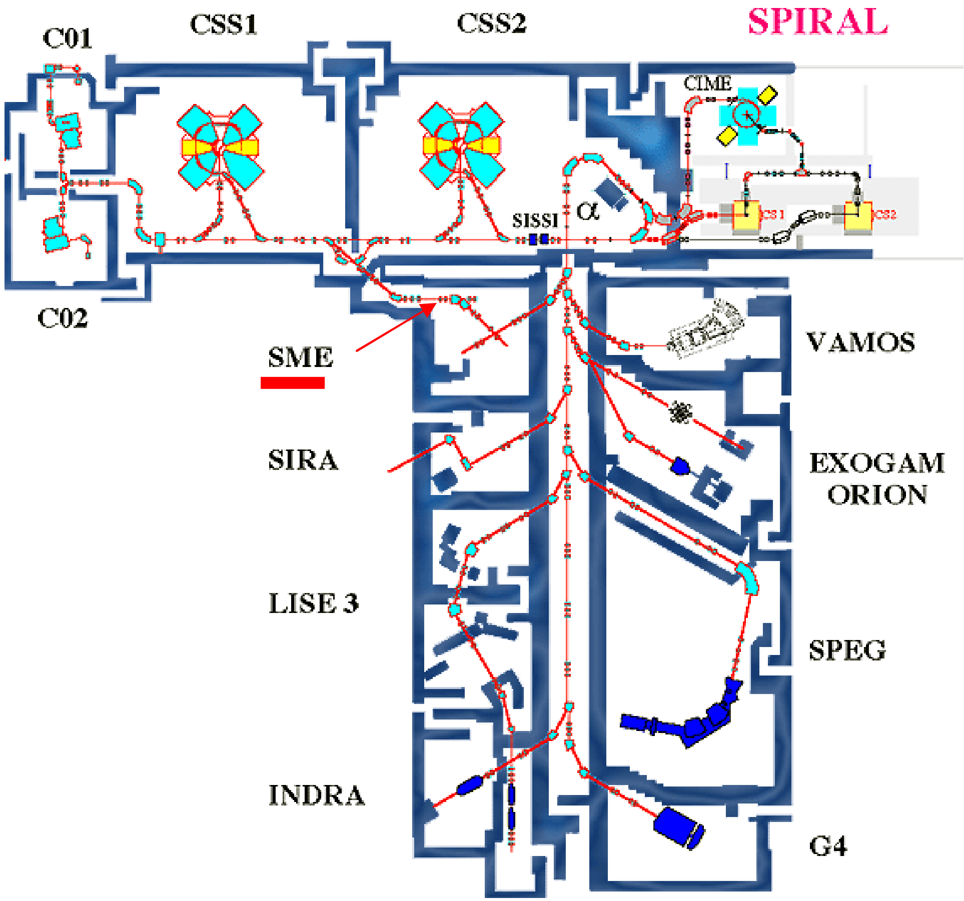

Installation des détecteurs

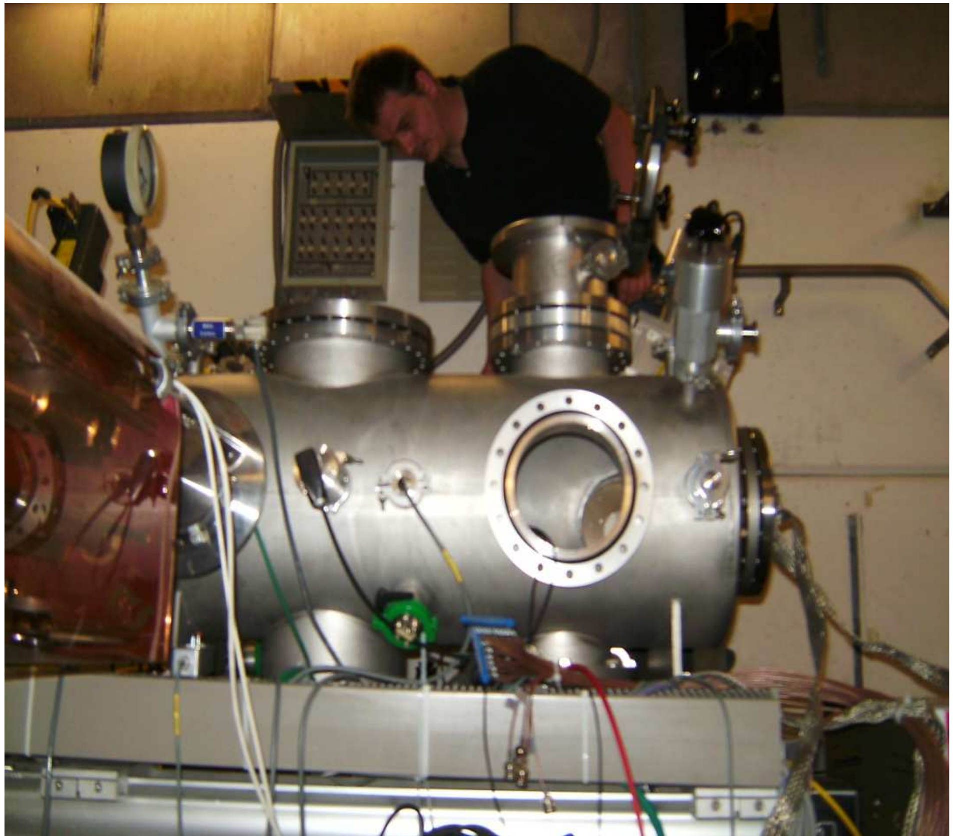

Table 4. Ions used in GANIL

Plaque + détecteur + alumine

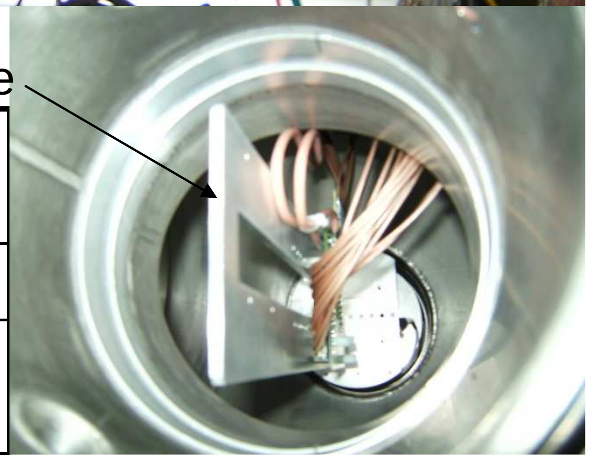

~2,5 m	GANIL ^{70}Zn	GANIL ^{36}S	GANIL ^{36}S	GANIL ^{16}O	LPC α
E/A (MeV)	8.7	7.2	3.9	13.7	1.2
Range (μ) ELS range (μ) ELP	63 55	48 42	26 22	225 198	15 13

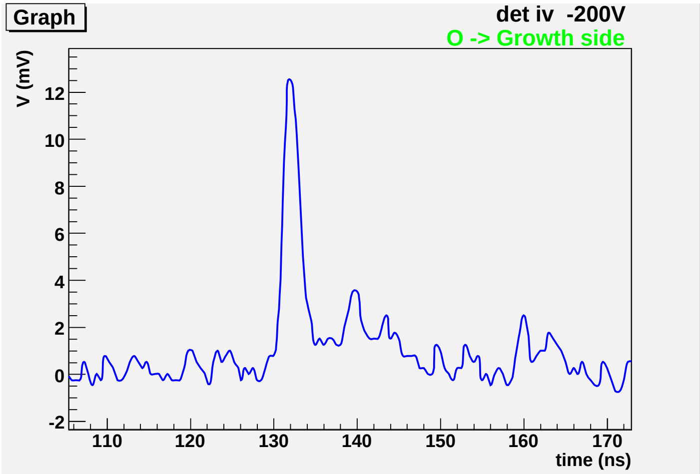

Det iv ELP, 350 µ, -200 V,
E=0.6V/µ board 3, channel 0;
O –> Growth side: 13.7 AMeV

S=18mm2; C=2,57 pF RC=0,13ns

Matacq -> 0,9 ns

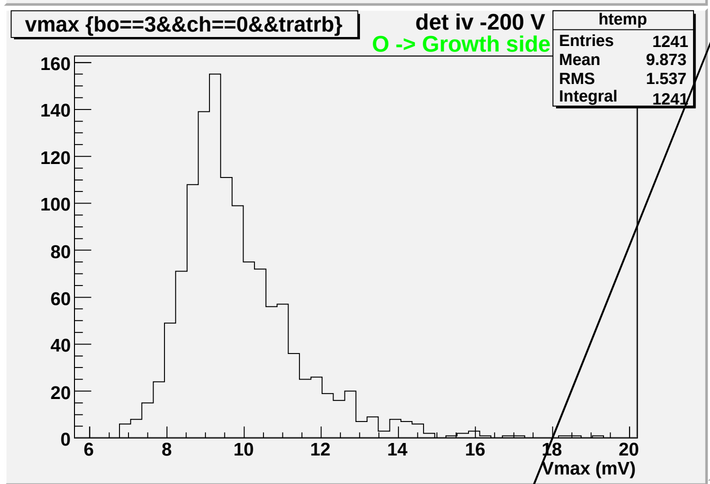

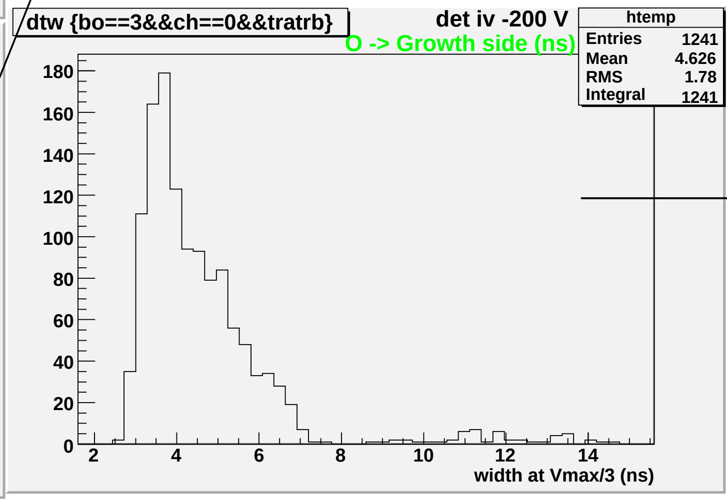

Calculated
Eeff < 0,25 V/µ

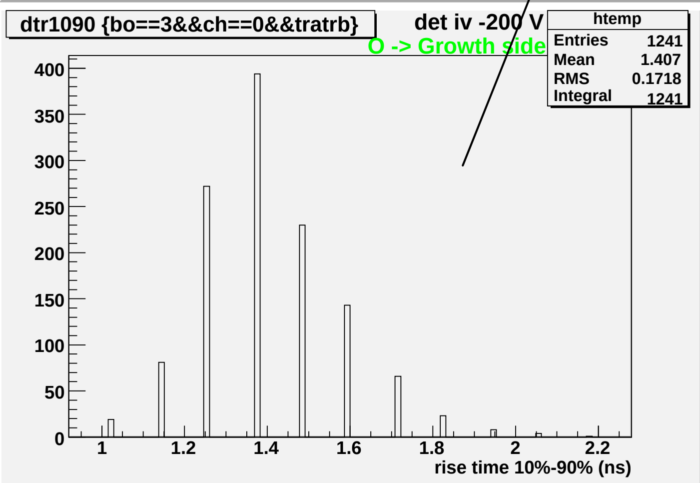

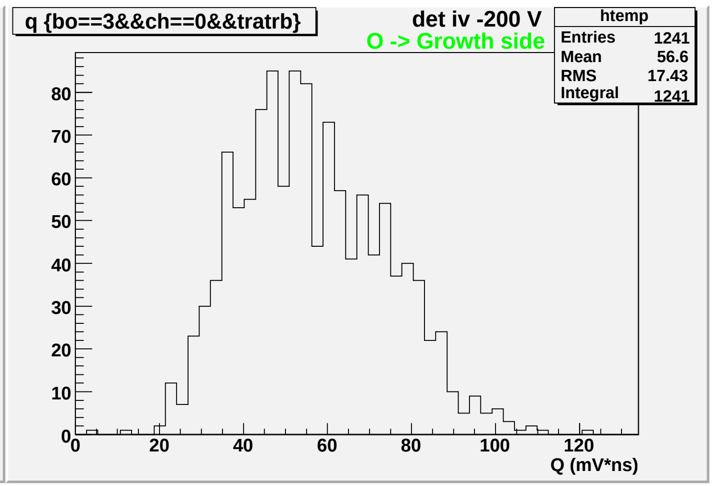

Acquisition:
MATACQ – VME (400 MHz BW; 2GHz sampling) – 12 channels
- oscillo LeCroy 64Xi (600 MHz BW; 10Gs/s) –
4 channels

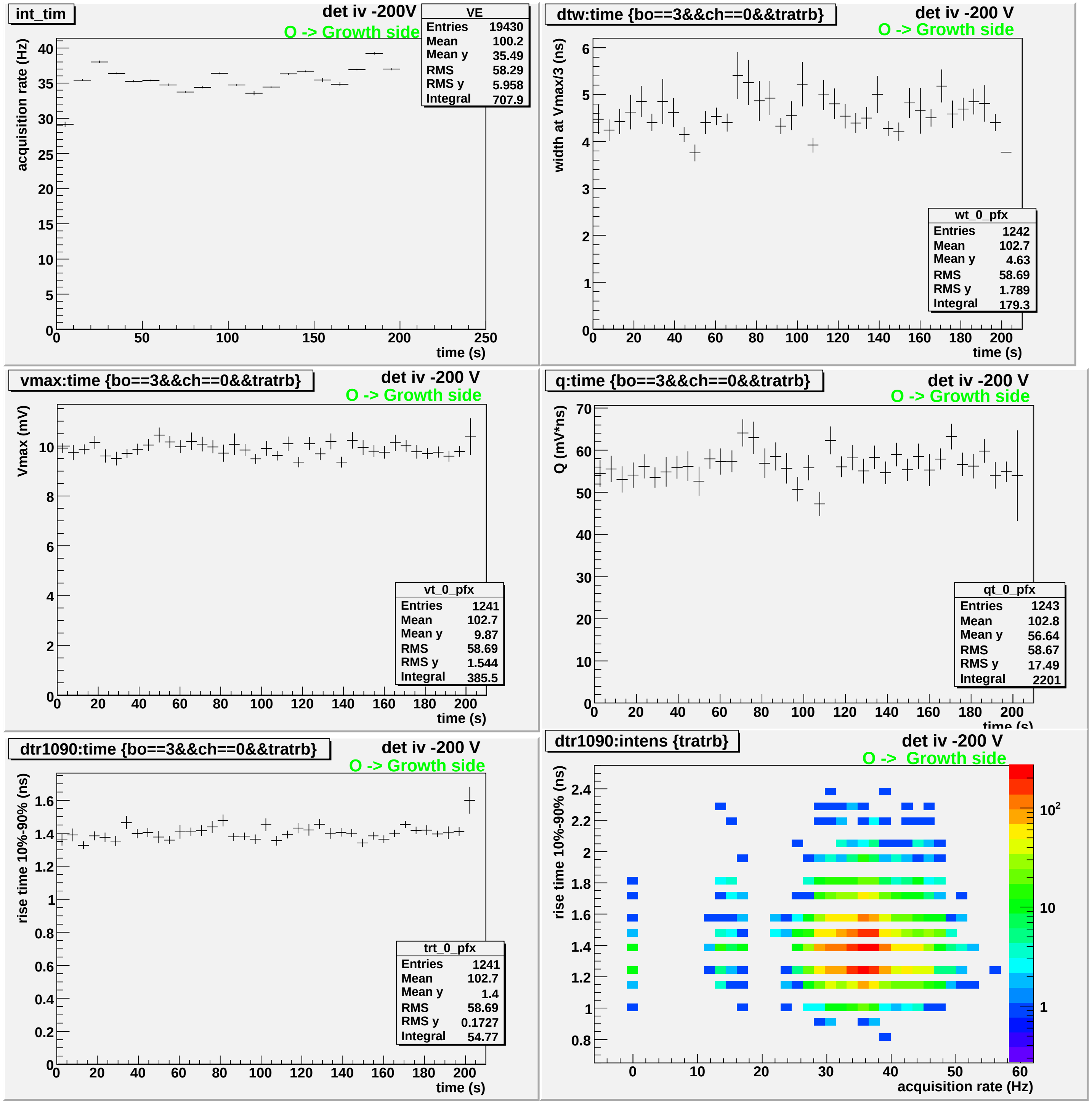

Det iv ELP, 350 µ
-200 V, E=0.6V/µ
board 3;
O: 13.7 AMeV

Det iv ELP, 350μ, -200 V, E=0.6V/μ, board 3; O:13.7 AMeV

the 4 channels of Matacq board 3 give similar results

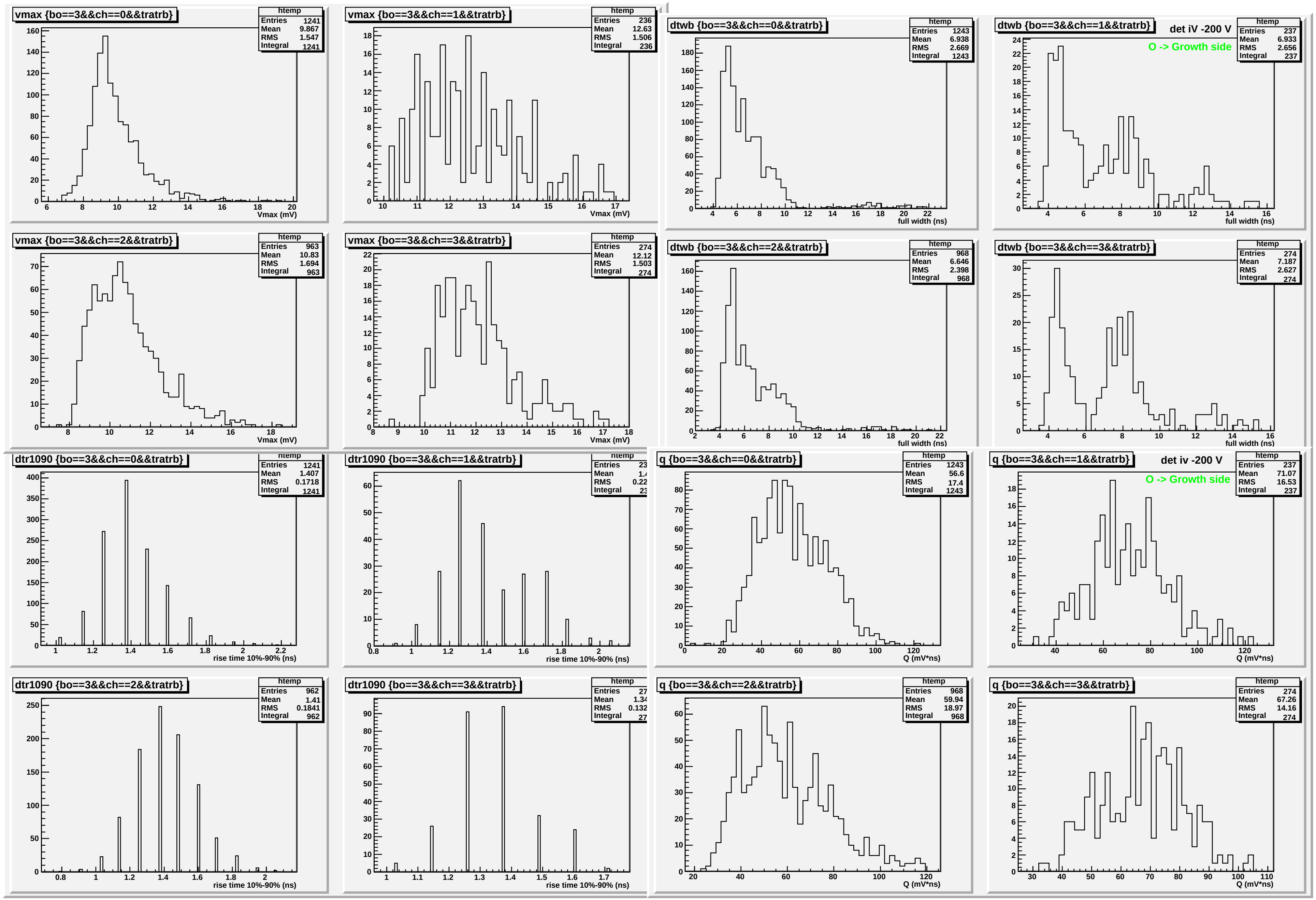

Det iv ELP, 350μ -200 V, E=0.6V/μ, board 3; O :13.7 AMeV

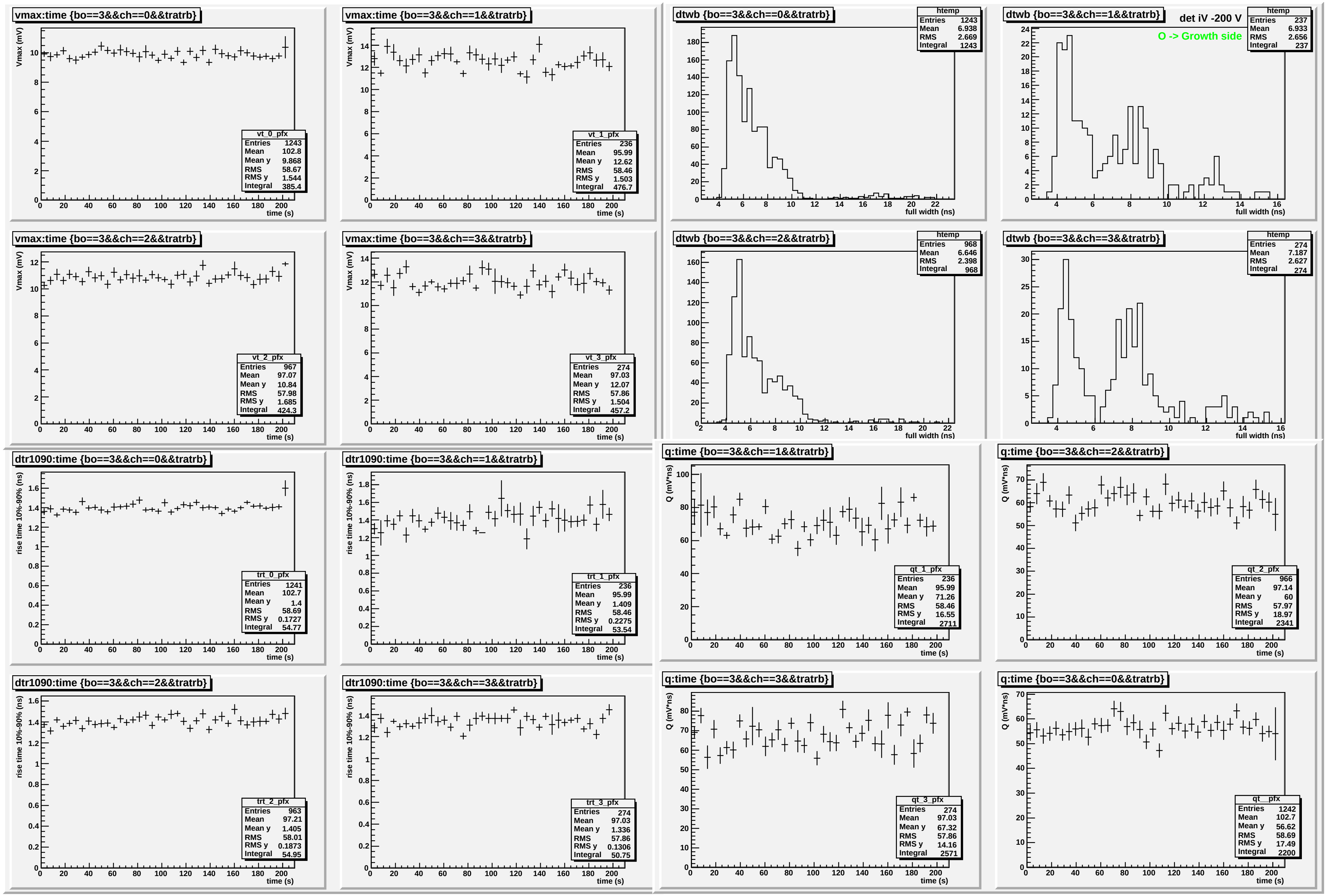

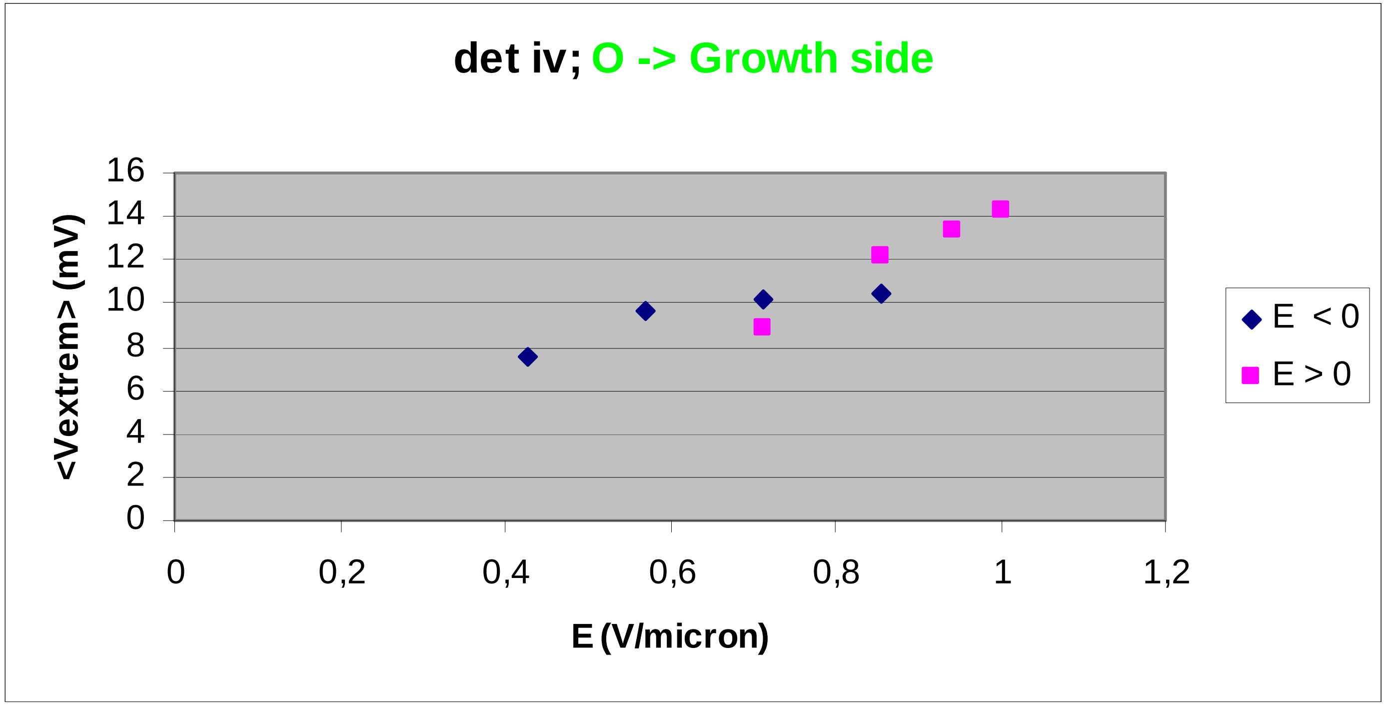
det iv; O -> Growth side
<Vextrem> (mV)
16
14
12
10
8
6
4
2
0
0
0,2
0,4
0,6
0,8
1
1,2
E (V/micron)
E < 0
E > 0

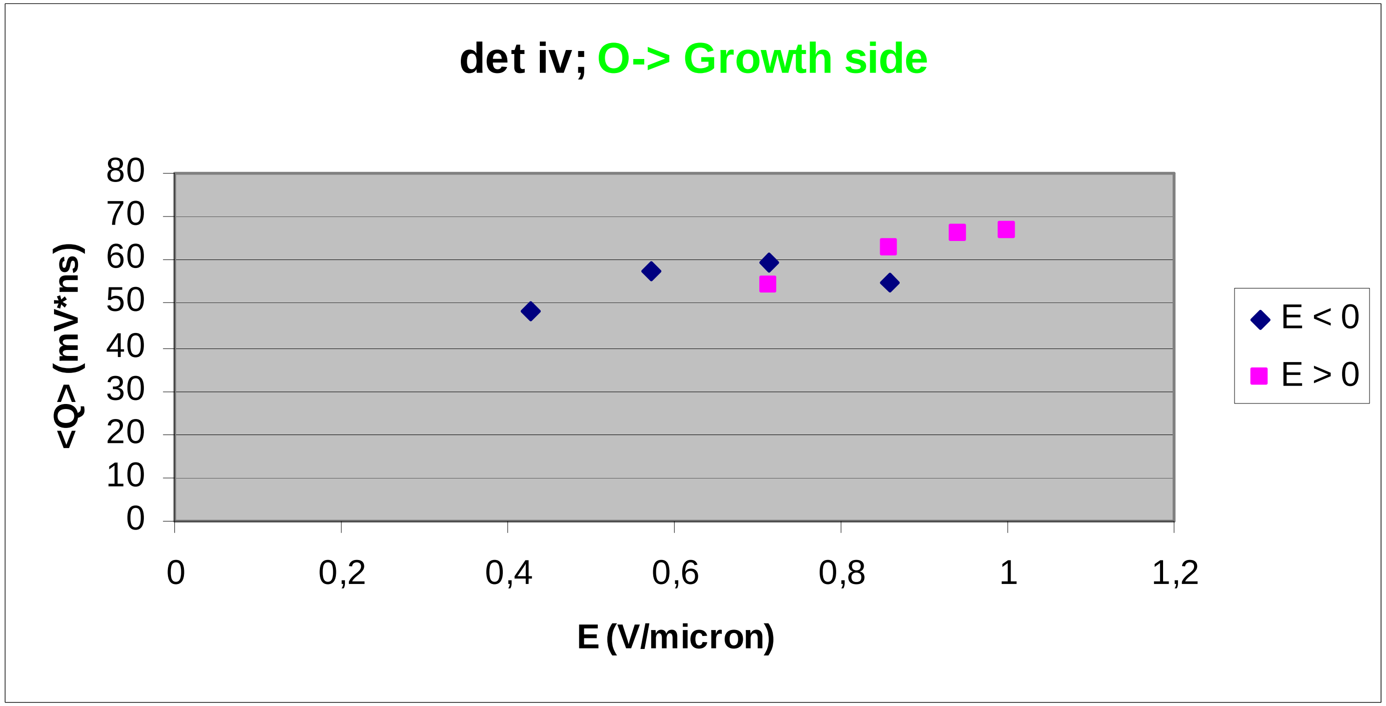
det iv; O-> Growth side
<Q> (mV*ns)
80
70
60
50
40
30
20
10
0
0
0,2
0,4
0,6
0,8
1
1,2
E (V/micron)
E < 0
E > 0

Résultats pour les détecteurs multipiste: *images prises sur l'oscilloscope LeCroy*

HT sur la face b) irradiée (1V/μ)

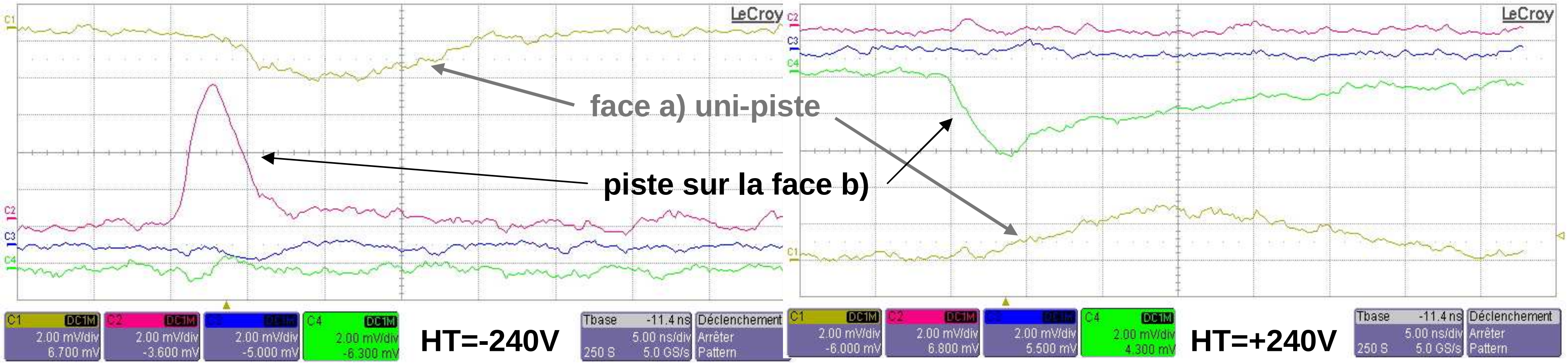

Signals induced by ^{36}S of 7.2 AMeV in the detector III of ELS type

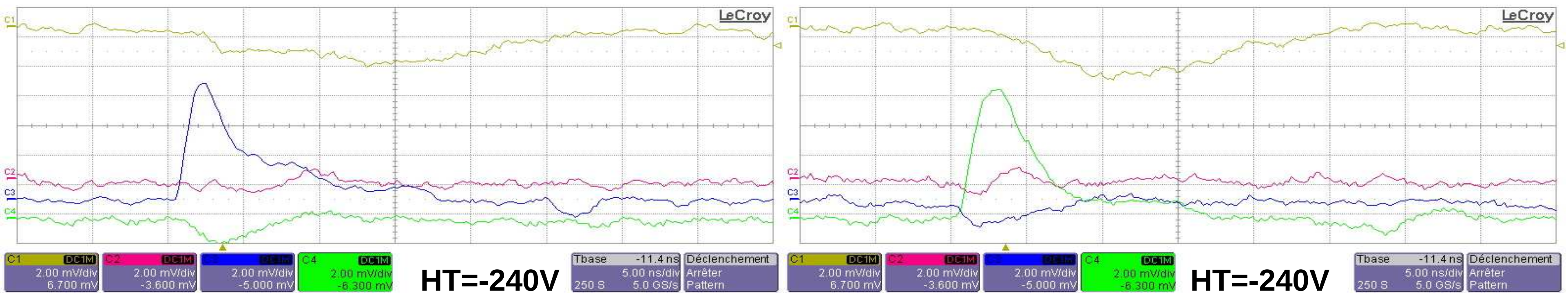

Signals induced by ^{36}S of 7.2 AMeV in the detector III of ELS type: examples of cross-talk between neighbouring strips on the irradiated face (blue and green)

Résultats pour les détecteurs multipiste: *images prises sur l’oscilloscope LeCroy*

Coincident signals on the two sides of the detector **HT sur la face a) irradiée (1V/µ)**

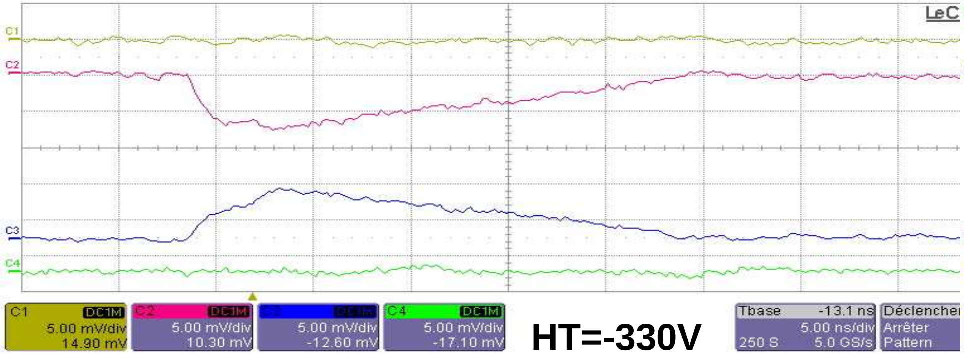

HT=-330V

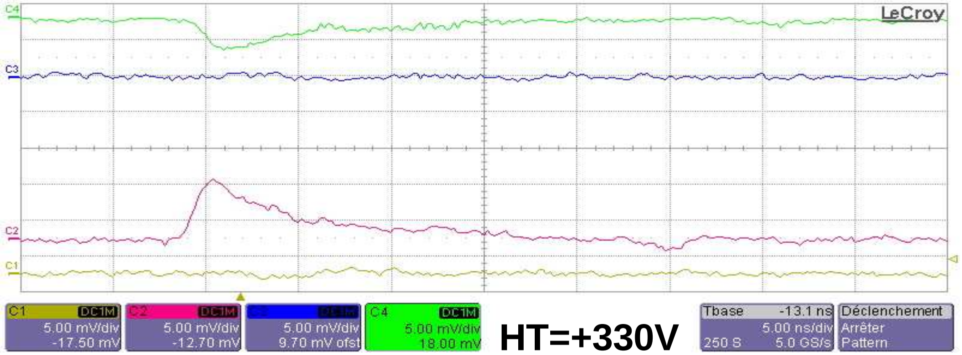

HT=+330V

Signals induced by ^{36}S of 7.2 AMeV in the detector IV of ELP type

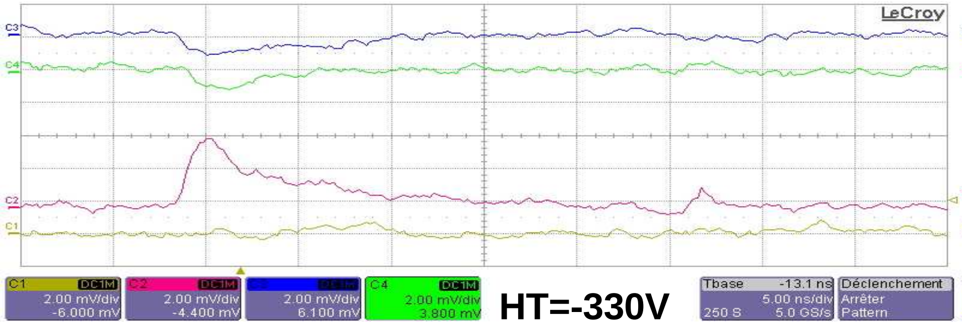

HT=-330V

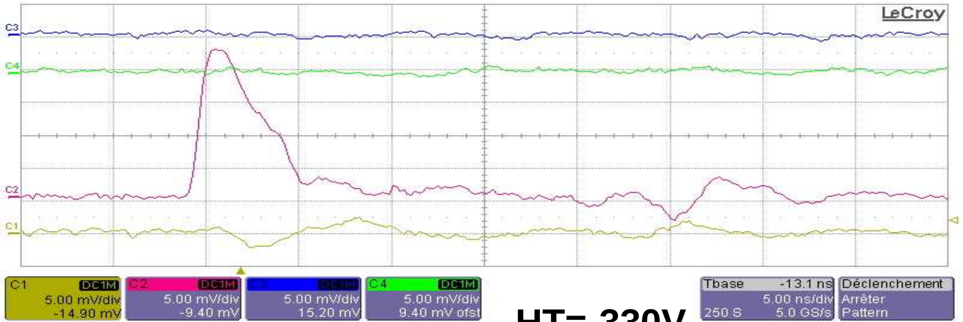

HT=-330V

The particle is probably passing between strips (left); example of cross-talk (right)

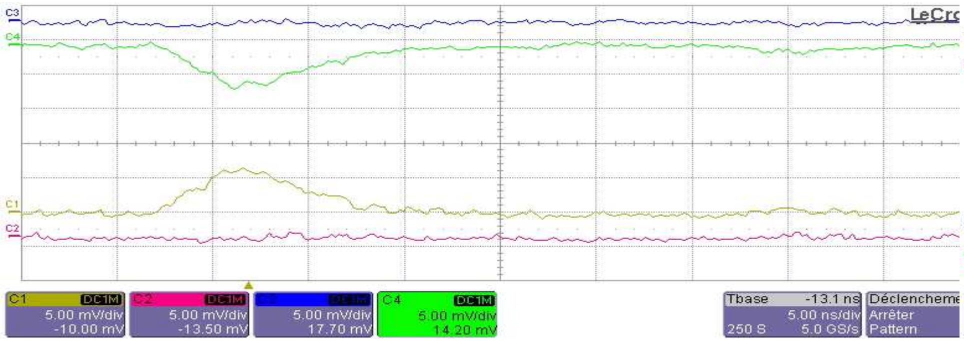

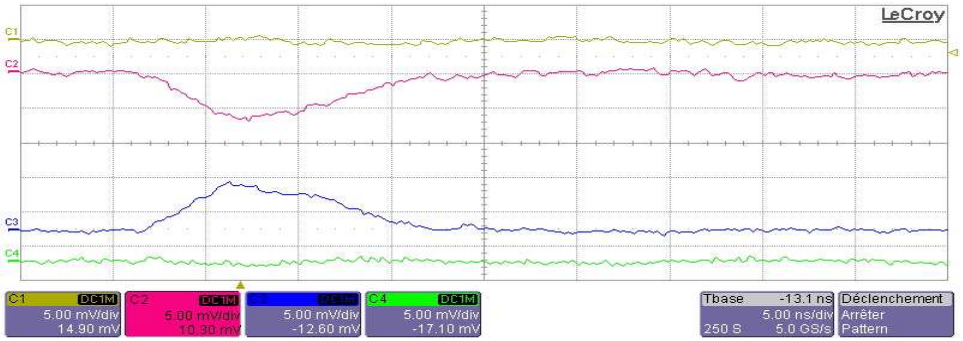

Signals induced by ^{36}S of 3.9 AMeV in the detector IV of ELP type (-330 V)

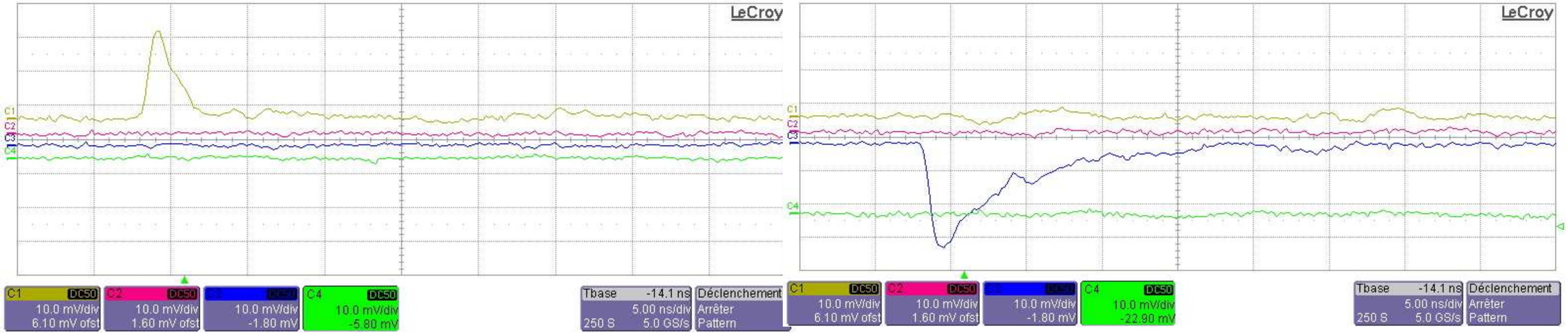

Signals from the strip no. 9 of the face a) - left (yellow curve) and from the strip 9 of the face b) - right (blue curve), amplified with the new preamplifier PRL developed at LPC; the signals were induced by the ^{70}Zn ions of 8.7 AMeV in the detector IV of ELP type for a voltage of -300 V applied on the face a) (growth), irradiated

Signaux coincidentes sur les deux faces du détecteur

HT sur la face a) irradiée (1V/μ)

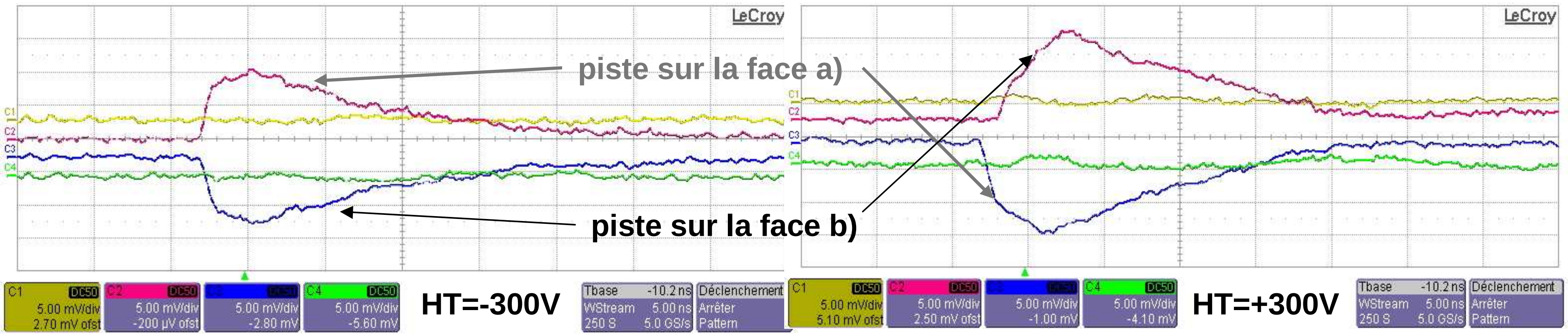

Signals induced by 70Zn of 8.7 AMeV in the detector IV of ELP type

V. Conclusions & prospective:

-**The CVD polycrystalline diamond based double sided strip detectors seems to be well suited to the requirements for a beam profiler for characterising low intensity radioactive heavy ion beams:**

- material: ELP (small bulk polarization; signal stable in time); P2 from Company 1, for example
- thickness: 200-300 µ adequate for R~50 µ
- electric field ~1V/µ; HV though Sh < Se
- strip: 1 mm pitch (0.9mm strip, inter-strip gap: 0.1mm), efficiency: 90-99% (localization with 1 mm resolution)
- small cross-talk effects
- signal shape study: ~1.5 ns rise time for 1 strip; PSA may bring interesting information ($\Delta Q < \Delta V_{extrem}$)

-**The further characterisation of such detectors and the engineering of the readout electronics and other associated elements of a fully fledged profiler are expected to be carried beyond the present study:**

- tests for radiation hardness

- double layer metallization: Ti,(Cr) Au to improve the contact and to avoid the ageing of Au film and its migration inside the diamond wafer;

- more robust electric contacts between PCB and strips?

- line receiver multi-channel preamplifiers for low energies

- acquisition system

-**Note:** The study of the diamond detector has been the subject for a Janus stage in 2008 (2 students), as well as of a TIPE presentation (3 students) and a M1 stage (1 student) in 2009.

References

[1] E.-K. Souw, R.J. Meilunas, Nucl. Instr. And Meth. In Phys. Res. A 400 (1997) 69.
[2] S. Schwertel et al., „Diamond detectors for the R3B Experiment", GSI Scientific Report 2007 (GSI Report 2008-1), Instruments-Methods-10, (2007) 216.
[3] P. Moritz, E. Bedermann, K. Blasche, H. Rodl, H. Stelzer, F. Zeytouni, DIPAC III, Frascati (1997).
[4] J.-L. Lecouey at al., Abstract n°. 226, ANIMMA, Marseille (2009).
[5] P.Bergonzo, D. Tromson, H. Hamrita, C. Mer, N. Tranchant, M. Nesladek, Diamond and Related Materials 16 (2007) 1038.
[6]A. Brauning-Demian, E. Bedermann, P. Verma and P.H. Mokler, DIPAC III, Frascati (1997).

We are in collaboration with:

GSI (Darmstadt): Angela Bräuning-Demian, Elèni Berdermann, M. Traeger, M. Ciobanu & Detector Laboratory

LIST (CEA Saclay): Hassen Hamrita, Philippe Bergonzo

NIPNE Bucharest: Dana Dimitriu, Daniela Fluerasu

LPC Caen:

Jean-Marc Fontbone, Jérôme Perronnel, Hervé Plard, Jean-François Cam

Jean Hommet – acquisition; Yvan Merrer – mécanique + atelier mécanique

Lynda Achouri, Nigel Orr, Marian Pârlog

Remerciements:

Fac. Chimie: M. Ledauphin CRISMAT: Yohann Thimont, Séverine Mouchel

IPN Lyon: Michel Chevalier

CIMAP: Emmanuel Balanzat, Jean-Marc Ramillon, Stéphane Guillos
LPC: Joel Brégéault, Jean-Louis Gabriel, Albert Leconte, Christophe Vandamme, l’équipe informatique